Conserved charge fluctuations and correlations in finite-density QCD

Frithjof Karsch
Bielefeld University

UNIVERSITÄT BIELEFELD
Faculty of Physics

- QCD phase diagram – constraining the location of a critical endpoint
- Higher order cumulants of net baryon-number fluctuations on the pseudo-critical line

CRC-TR 211 Strong-interaction matter under extreme conditions
DFG Deutsche Forschungsgemeinschaft

Exploring the phase diagram of strong-interaction matter

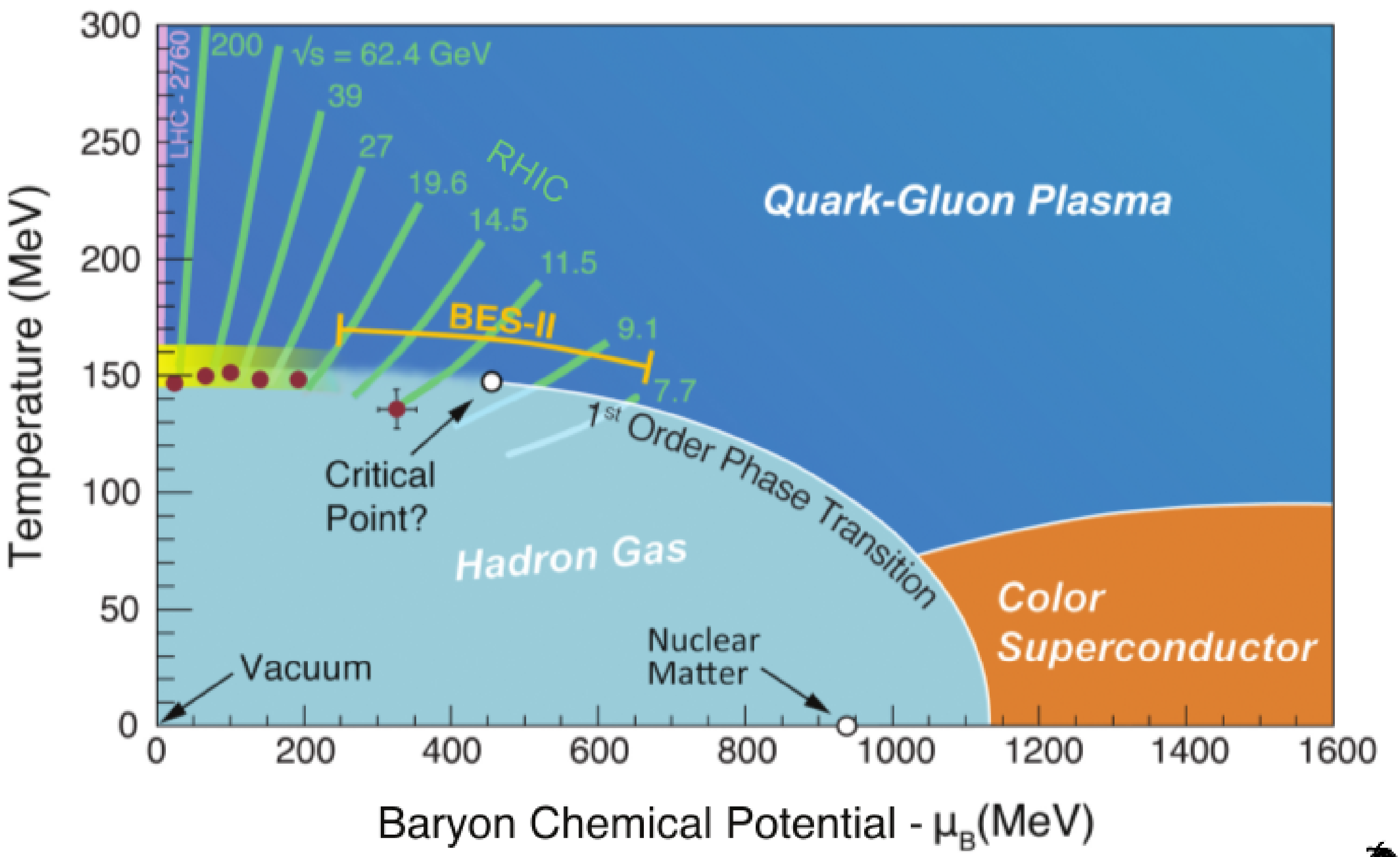

Where is the
critical point?

Pseudo-critical line for physical quark mass values

$$T_{pc}(\mu_B) = T_{pc}(0)\left(1 - \kappa_2\left(\frac{\mu_B}{T_{pc}(\mu_B)}\right)^2 - \kappa_4\left(\frac{\mu_B}{T_{pc}(\mu_B)}\right)^4 + \dots\right)$$

phase diagram at physical values of the quark masses

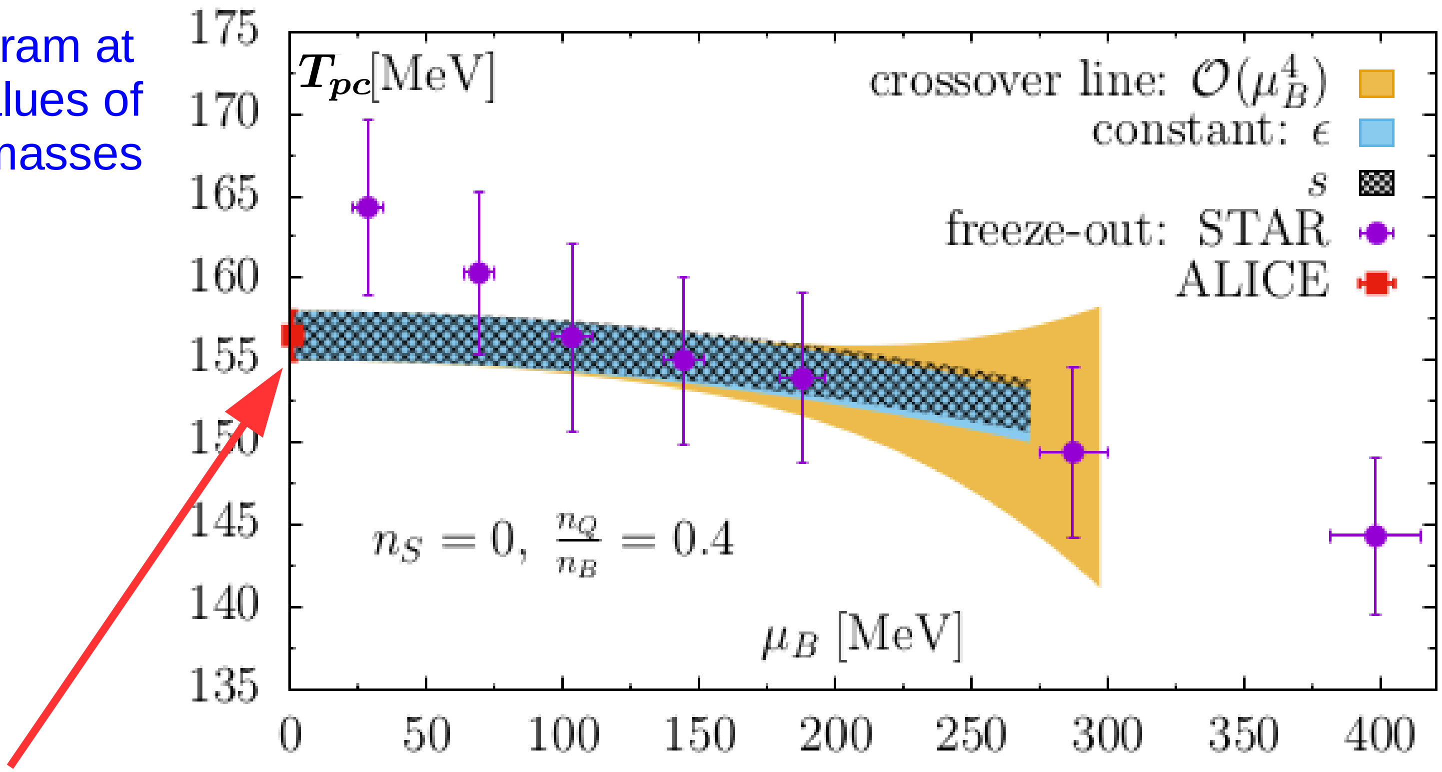

STAR: arXiv:1701.07065

A. Andronic et al., Nature 561 (2018) 321

$T_{pc} = (156.5 \pm 1.5)$ MeV

$\kappa_2 = 0.012(4)$

$\kappa_4 = 0.000(4)$

A. Bazavov et al. [HotQCD], Phys. Lett. B795 (2019), arXiv:1812.08235

$T_{pc} = (158.0 \pm 0.6)$ MeV

$\kappa_2 = 0.0153(18)$

$\kappa_4 = 0.00032(67)$

S. Borsanyi, et al, PRL 125 (2020) arXiv:2002.02821

Phases of strong-interaction matter

determination of T_c^0 puts an upper limit on T^{CEP}

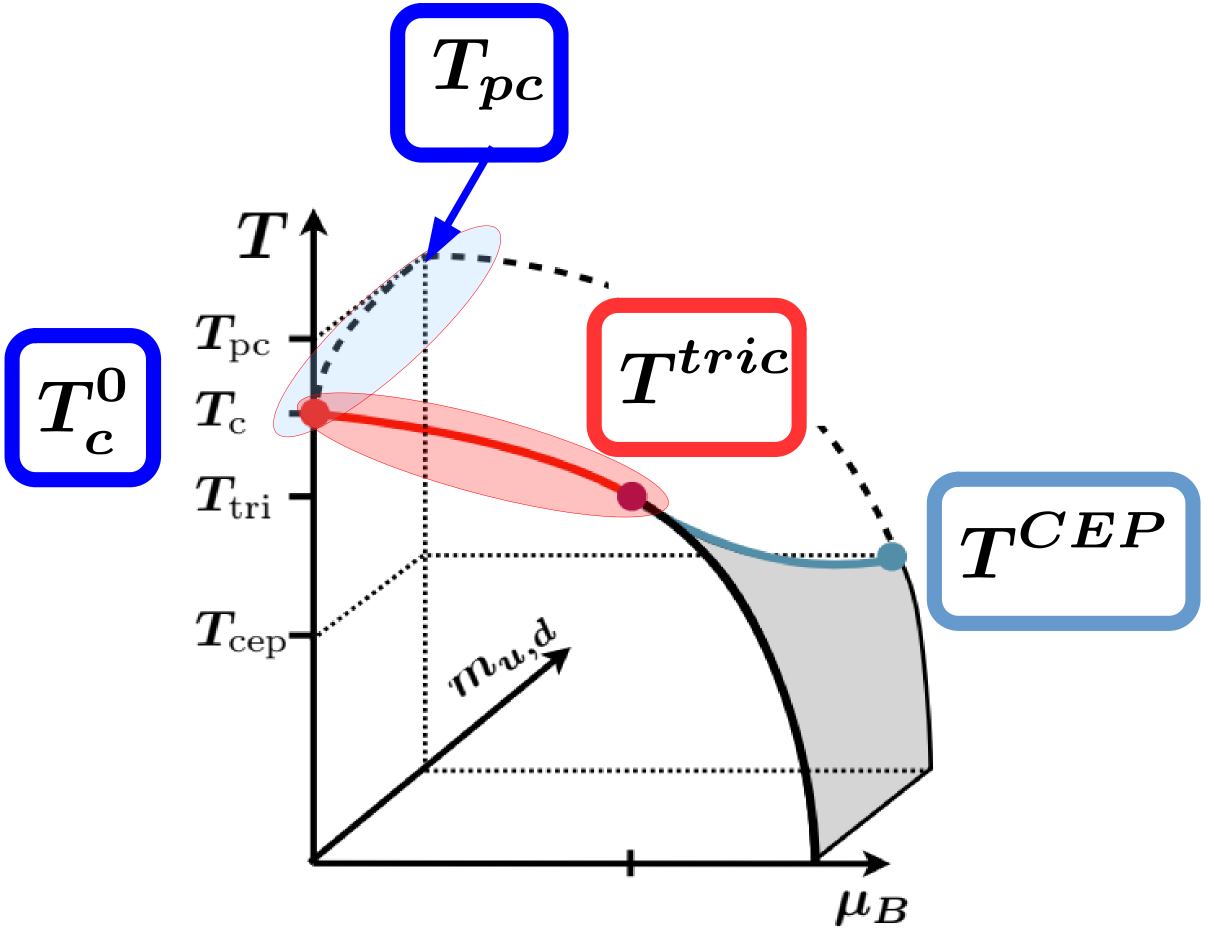

pseudo-critical temperatures from maxima of "appropriate" susceptibilities
– no unique definition –

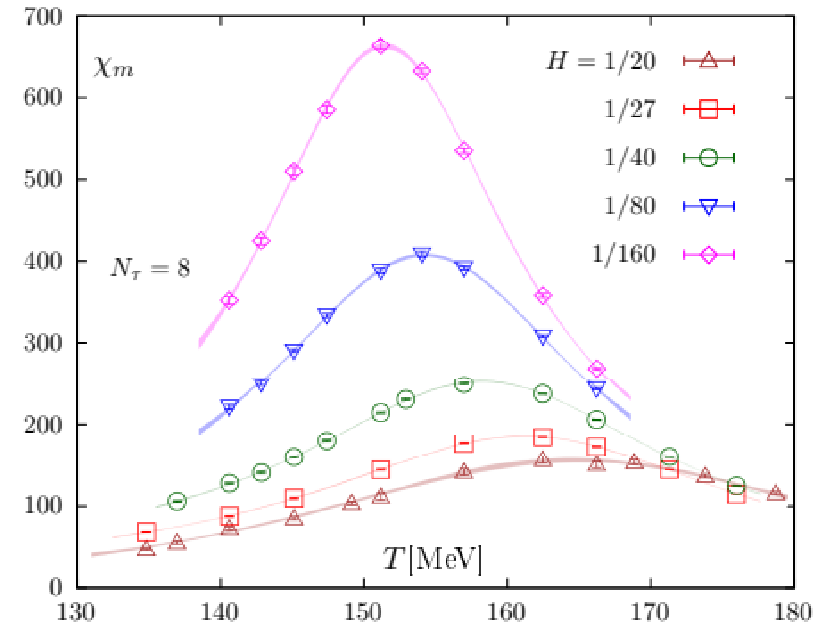

$$H = m_\ell / m_s$$

$$m_\pi = (160 - 55)\mathrm{MeV}$$

Random Matrix Model — A. Halasz, A.D. Jackson, R.E. Shrock, M.A. Stephanov, J.J.M. Verbaarschot, Phys. Rev. D58 (1998) 096007

QCD motivated — M. Stephanov, Phys. Rev. D73 (2006) 094508

NJL — M. Buballa, S. Carignano, Phys. Lett. B791 (2019) 361

Pseudo-critical and critical temperatures

$$T_{pc}(H) = T_c + z_x T_c H^{1/\beta\delta} \quad , \quad x = \text{peak}, \delta, ...$$

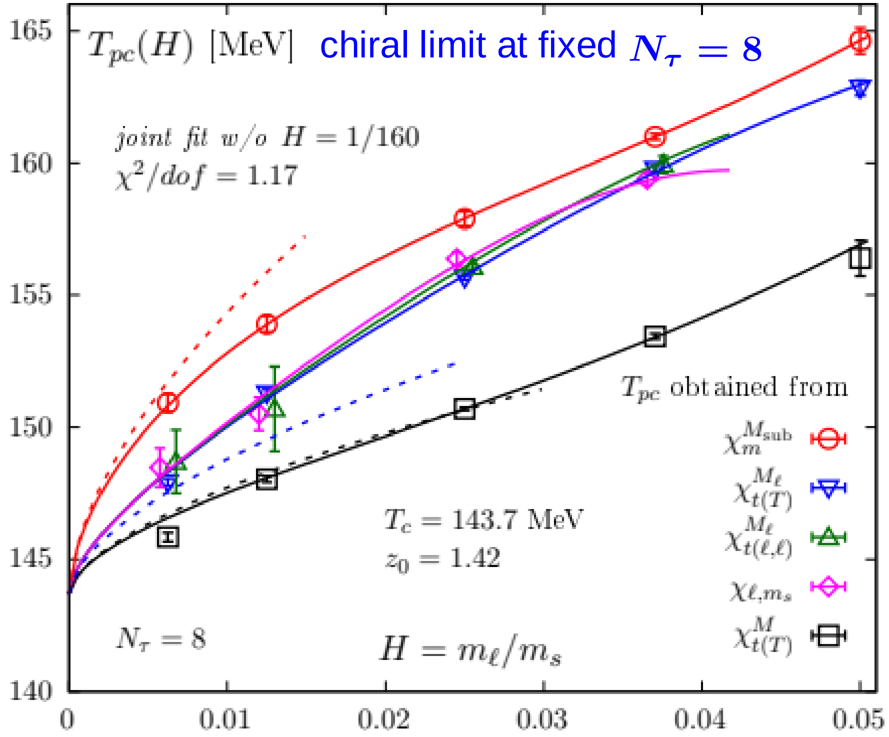

H.T.Ding, O. Kaczmarek, FK, P. Petreczky, Mugdha Sarkar, C. Schmidt, Sipaz Sharma, arXiv:2403.09390

physical masses

T_δ : T at ~60% of peak height

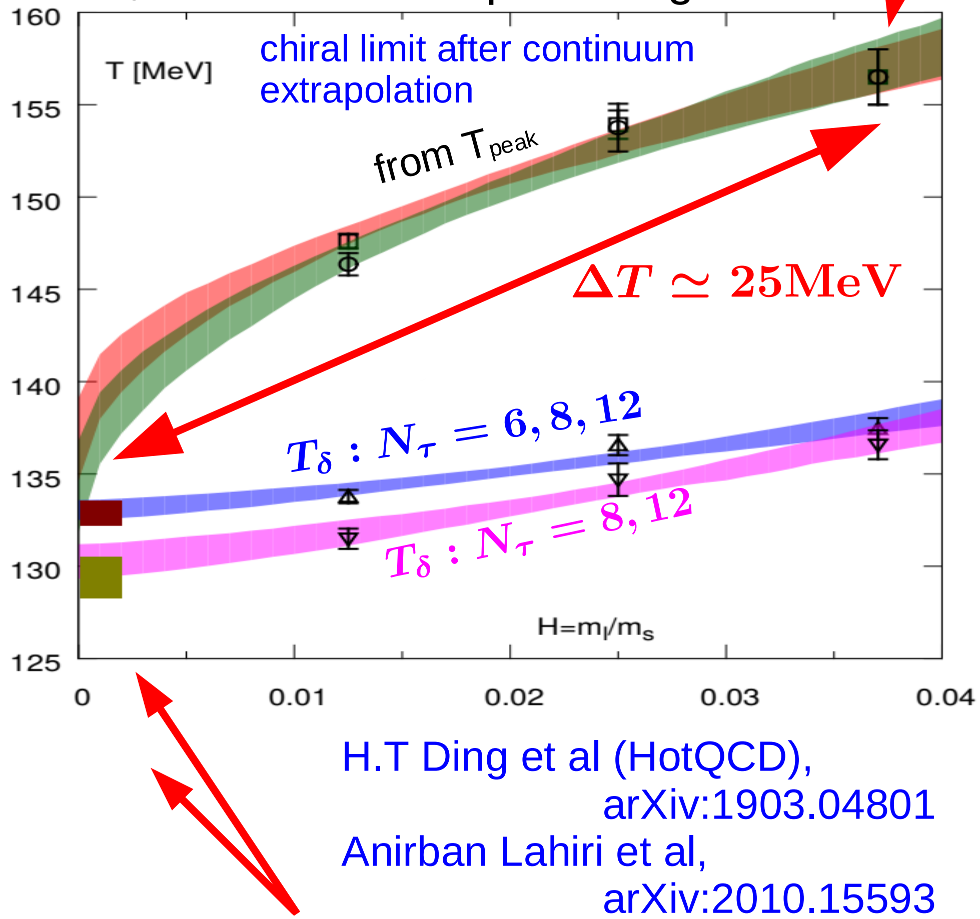

H.T Ding et al (HotQCD), arXiv:1903.04801

Anirban Lahiri et al, arXiv:2010.15593

physical masses

$$T_{pc}^{phys} = (156.5 \pm 1.5) \text{ MeV}$$

A. Bazavov et al (HotQCD), arXiv:1812.08235

chiral limit extrapolations

$$T_c^0 = 132^{+3}_{-6} \text{ MeV}$$

also: A. Y. Kotov et al., arXiv: 2105.09842

Phases of strong-interaction matter

determination of T_c^0 puts an upper limit on T^{CEP}

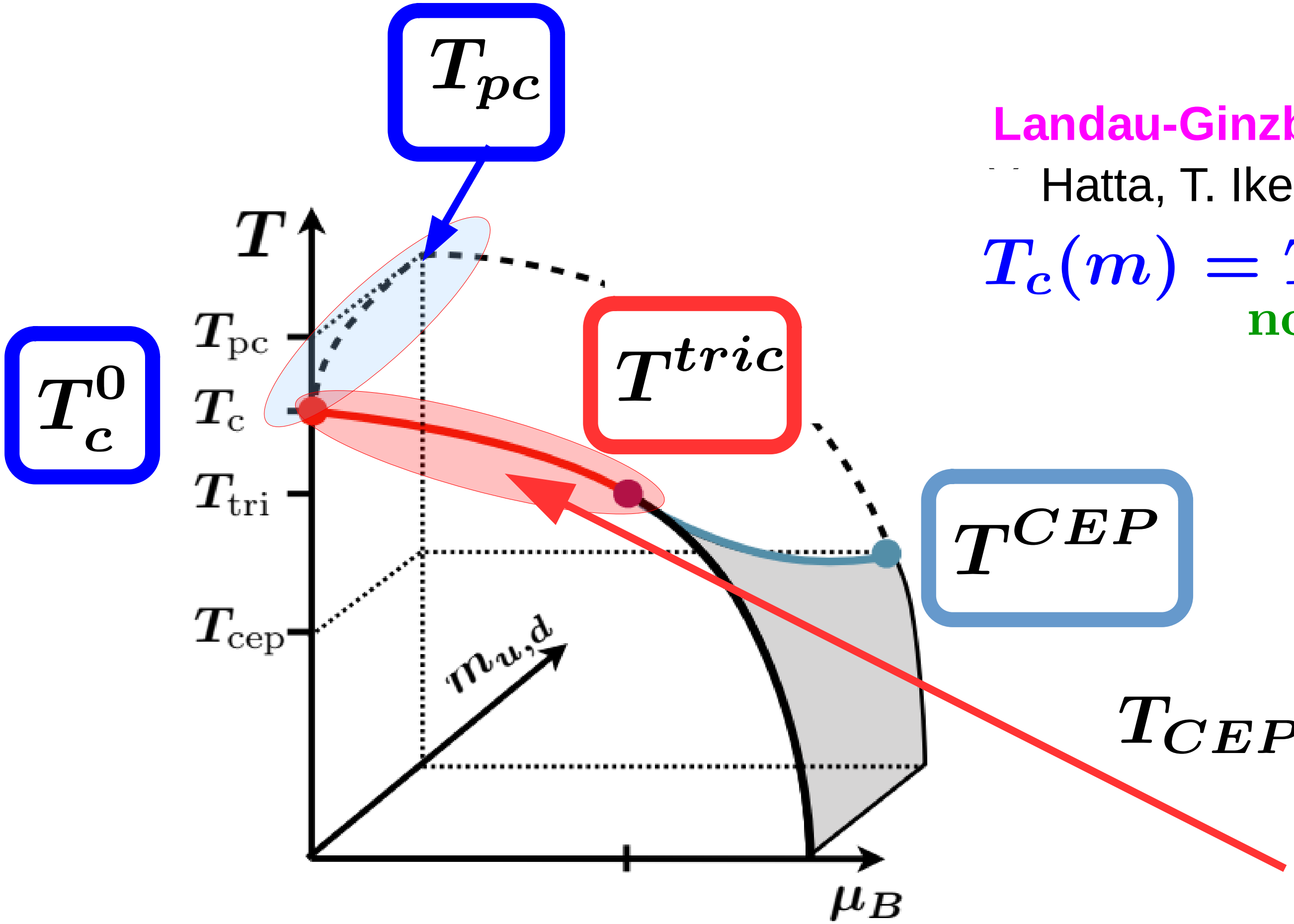

Landau-Ginzburg potential:

Hatta, T. Ikeda, Phys. Rev. D67 (2003) 014028

$$T_c(m) = T^{tric} - c\ m^{2/5}$$

$$\mathrm{non-universal,\ \ but\ c > 0}$$

$$T_{CEP} < T^{tric} < T_c^0 < T_{pc}^0$$

curvature in the chiral limit;
weak quark mass dependence:

H.-T. Ding et al. PRD 109 (2024) 114516

Random Matrix Model — A. Halasz, A.D. Jackson, R.E. Shrock, M.A. Stephanov, J.J.M. Verbaarschot, Phys. Rev. D58 (1998) 096007

QCD motivated — M. Stephanov, Phys. Rev. D73 (2006) 094508

NJL — M. Buballa, S. Carignano, Phys. Lett. B791 (2019) 361

The critical surface at non-zero density
– curvature of critical lines in the chiral limit –

– rather then using the **conserved charge basis**
we may switch to the **conserved flavor basis**

$$\Big\} (\mu_B, \mu_S) \Rightarrow (\mu_\ell, \mu_s)$$

$$\mu_\ell = \mu_B/3$$
$$\mu_s = \mu_B/3 - \mu_S$$

$$T_{pc,x}(\mu_\ell, \mu_s) = T_c \left(1 - (\kappa_2^\ell \mu_\ell^2 + \kappa_2^s \mu_s^2 + 2\kappa_{11}^{\ell s} \mu_\ell \mu_s)/T^2 + \frac{z_x}{z_0} H^{1/\beta\delta}\right)$$

$$\mathcal{K}_2^f(T) = \frac{1}{2T_c} \left(\frac{T^2 \partial^2 M_\ell / \partial \mu_f^2}{\partial M_\ell / \partial T}\right)_{(T,0)}$$

$$\mathcal{K}_{11}^{\ell s}(T) = \frac{1}{2T_c} \left(\frac{T^2 \partial^2 M_\ell / \partial \mu_\ell \partial \mu_s}{\partial M_\ell / \partial T}\right)_{(T,0)}$$

$$\Bigg\} \quad \kappa_2^f \equiv \mathcal{K}_2^f(T_c) \ , \quad f = \ell,\ s$$
$$\kappa_{11}^{\ell s} \equiv \mathcal{K}_{11}^{\ell s}(T_c)$$

⇓

$$\kappa_2^B = \frac{1}{9}\left(\kappa_2^\ell + 2\kappa_2^{\ell s} + \kappa_2^s\right)$$

$$\kappa_2^S = \kappa_2^s$$

$$\kappa_{11}^{BS} = -\frac{1}{3}\left(\kappa_2^s + \kappa_2^{\ell s}\right)$$

Curvature of the critical surface

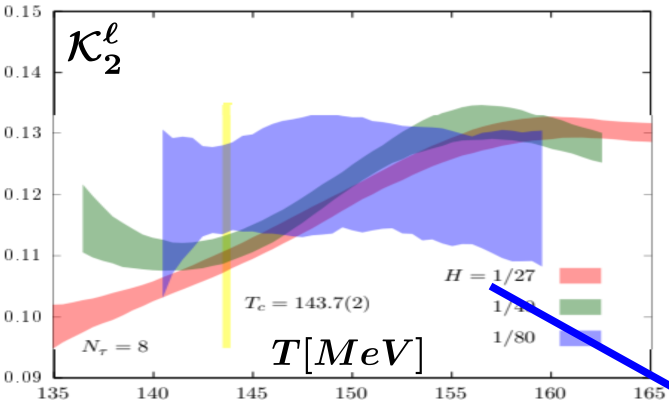

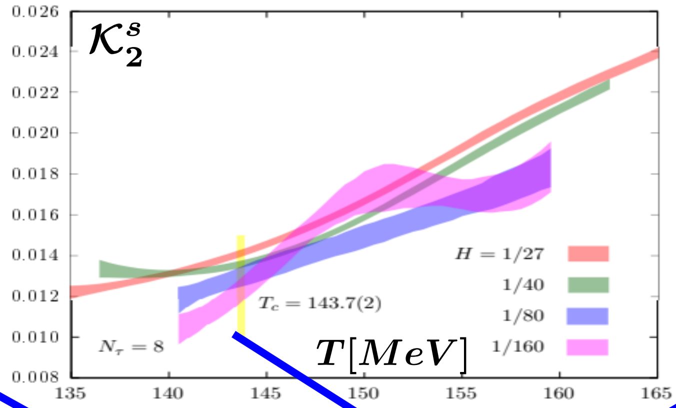

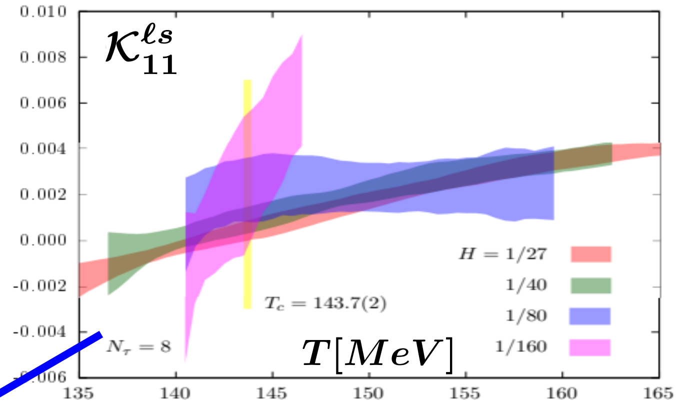

$$\kappa_2^B = \frac{1}{9}\left(\kappa_2^\ell + 2\kappa_2^{\ell s} + \kappa_2^s\right)$$

$$\kappa_2^S = \kappa_2^s$$

$$\kappa_{11}^{BS} = -\frac{1}{3}\left(\kappa_2^s + \kappa_2^{\ell s}\right)$$

Note:

$\kappa_2^\ell \simeq (8-10)\kappa_2^s > 0$

$\kappa_{11}^{\ell s} \simeq 0$

$\kappa_{11}^{BS} \simeq -\frac{1}{3}\kappa_2^s < 0$

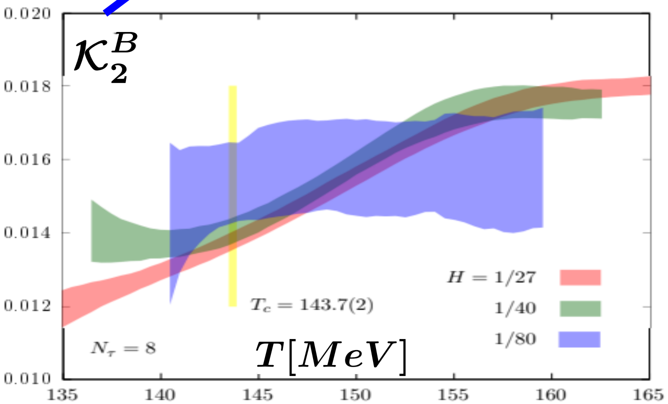

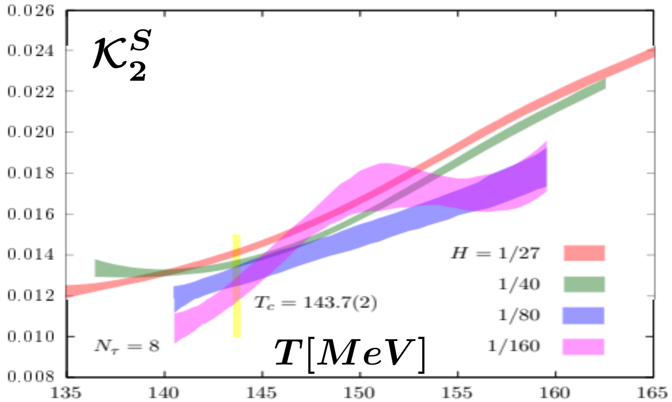

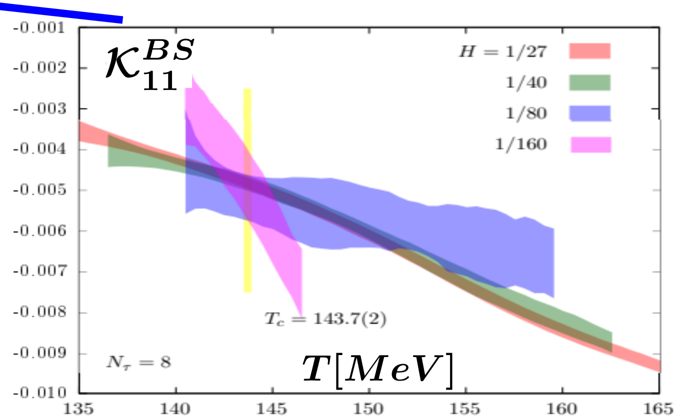

HotQCD – Mugdha Sarkar et al, PRD 109 (2024) 114516

The critical surface in the $\mu_B - \mu_S$ plane

$$\kappa_2^{\mu_S=0} > \kappa_2^{n_S=0} > \kappa_2^{\mu_s=0}$$

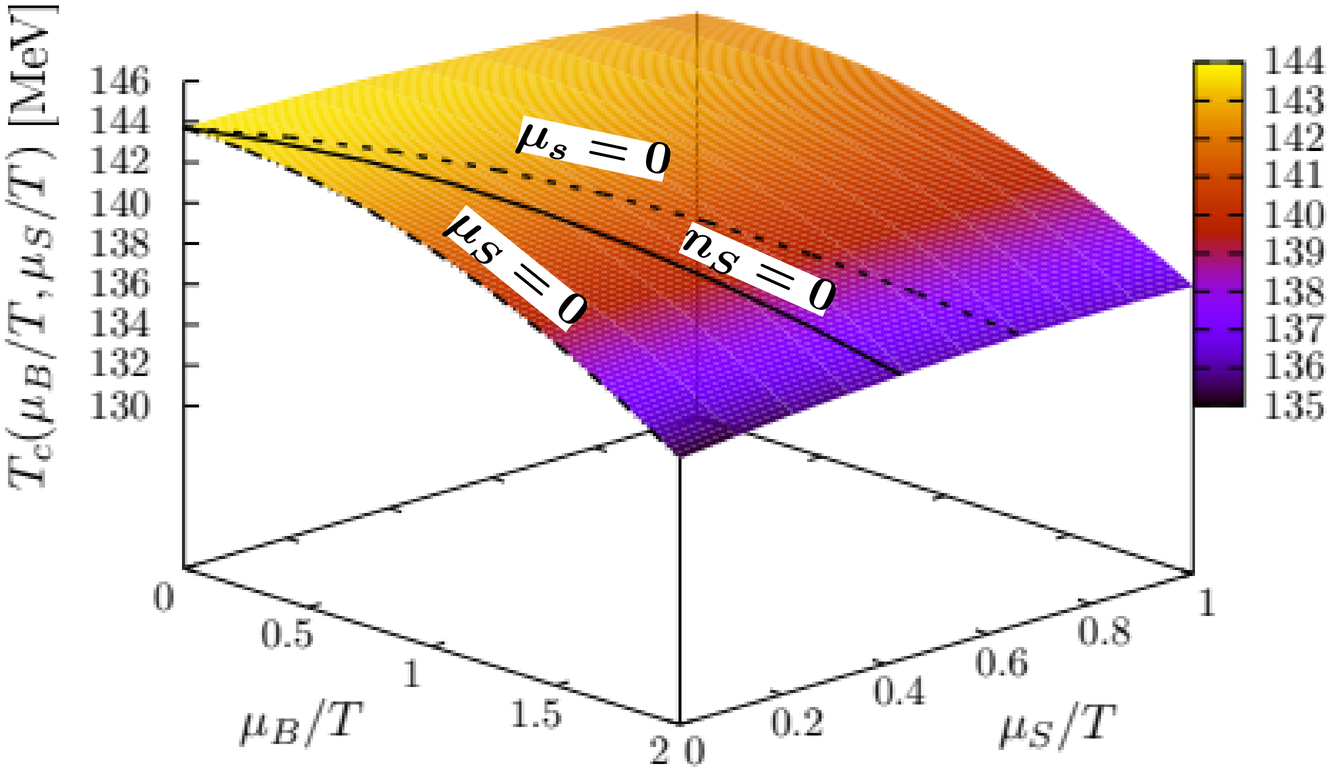

$$\mu_S = 0: \quad \kappa_2^{\mu_S=0} = \kappa_2^B = 0.015(1)$$

$$n_S = 0: \quad \kappa_2^{n_S=0} = \kappa_2^B \left(1 + s_1^2 \frac{\kappa_2^S}{\kappa_2^B} + 2s_1 \frac{\kappa_{11}^{BS}}{\kappa_2^B}\right) = 0.895(31)\kappa_2^B$$

$$\mu_s = 0: \quad \kappa_2^{\mu_s=0} = \kappa_2^B \left(1 + \frac{1}{9} \frac{\kappa_2^S}{\kappa_2^B} + \frac{2}{3} \frac{\kappa_{11}^{BS}}{\kappa_2^B}\right) = 0.972(19)\kappa_2^{n_S=0}$$

determination of T_c^0 puts an upper limit on T^{CEP}

$T_{pc} = 156.5(1.5)\mathrm{MeV}$

$T_c^0 = 132^{+3}_{-6}\mathrm{MeV}$

A. Bazavov et al (HotQCD), arXiv:1812.08235

H.T. Ding et al (HotQCD), arXiv:1903.04801

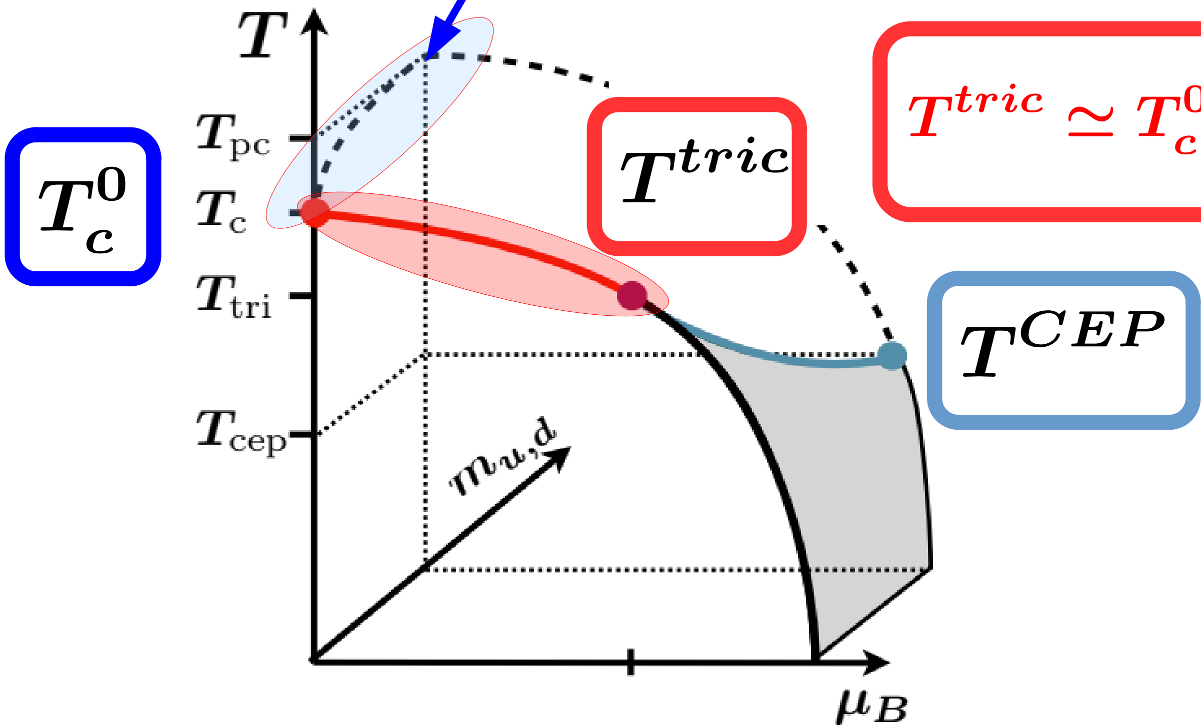

$$T^{tric} \simeq T_c^0 - 1.9(6)\ \mathrm{MeV} \left(\frac{\mu_B}{T_c}\right)^2_{tric}$$

Taylor series suggests

$(\mu_B/T)_{tric} \geq 2$

$T^{CEP} < T^{tric} < T_c^0$

$$T^{CEP} < 125\ \mathrm{MeV}$$

the temperature range below T_c^0 is most important for getting information on a possible CEP

upper limit on T^{CEP} puts constraint on HIC searches for the CEP

– pseudo-critical temperatures at physical quark mass values

$$T_{pc}(\mu_B) = 156.5(1.5)\mathrm{MeV}\left(1 - 0.012(4)\left(\frac{\mu_B}{T}\right)^2 - / + \dots\right)$$

⇨ to reach $T < 125\mathrm{MeV}$ $T < 110\mathrm{MeV}$

need $\mu_B/T \simeq 4$ $\mu_B/T \simeq 5$

$\mu_B \geq 500\mathrm{MeV}$ $\mu_B \gtrsim 550\mathrm{MeV}$

my extrap.

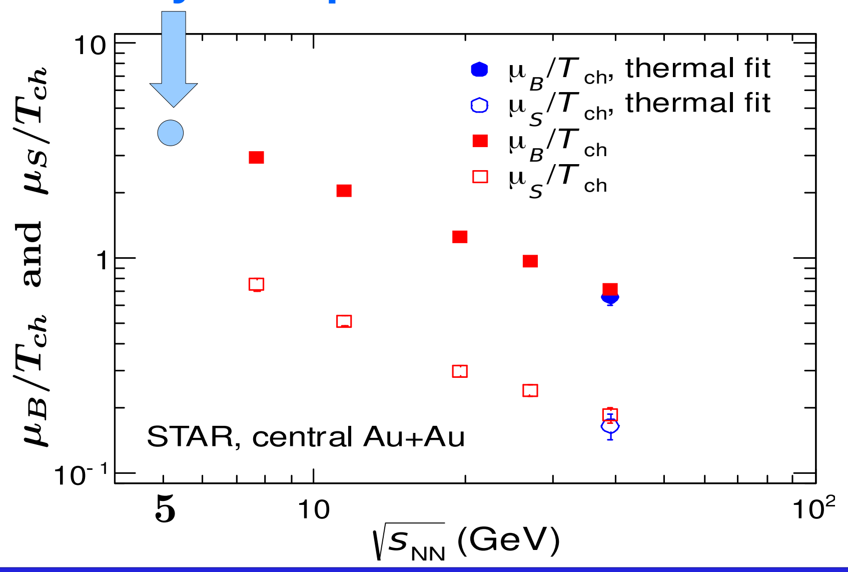

Search for the Critical End Point requires beam energies

$$\sqrt{s_{NN}} \leq 5\ \mathrm{GeV}$$

STAR freeze-out parameter, arXiv:1906.03732
also: HADES collaboration, arXiv:1512.07070

QCD thermodynamics at non-zero net baryon-density
– Taylor expansion –

Taylor expansion of the QCD pressure: $\frac{P}{T^4} = \frac{1}{VT^3} \ln Z(T, V, \mu_B, \mu_Q, \mu_S)$

$$\frac{P}{T^4} = \sum_{i,j,k=0}^{\infty} \frac{1}{i!j!k!} \chi_{ijk}^{BQS}(T) \left(\frac{\mu_B}{T}\right)^i \left(\frac{\mu_Q}{T}\right)^j \left(\frac{\mu_S}{T}\right)^k$$

cumulants of net-charge fluctuations and correlations:

$$\chi_{ijk}^{BQS} = \left. \frac{\partial^{i+j+k} P/T^4}{\partial \hat{\mu}_B^i \partial \hat{\mu}_Q^j \partial \hat{\mu}_S^k} \right|_{\mu_{B,Q,S}=0} \quad , \quad \hat{\mu}_X \equiv \frac{\mu_X}{T}$$

constrained Taylor series, demanding strangeness neutrality: $n_S = 0$

and: $n_Q/n_B = 0.4$

$$\begin{aligned} \hat{\mu}_Q(T, \mu_B) &= q_1(T)\, \hat{\mu}_B + q_3(T)\, \hat{\mu}_B^3 + \mathcal{O}(\hat{\mu}_B^5) \\ \hat{\mu}_S(T, \mu_B) &= s_1(T)\, \hat{\mu}_B + s_3(T)\, \hat{\mu}_B^3 + \mathcal{O}(\hat{\mu}_B^5) \end{aligned}$$

$$\frac{P}{T^4} = \sum_{k=0}^{\infty} \frac{1}{k!} \tilde{\chi}_k^B(T) \left(\frac{\mu_B}{T}\right)^k$$

C. Allton ...S.Ejiri...FK,
Phys.Rev.D 71 (2005) 054508

Up to 8th order cumulants are used "frequently" – Taylor expansion –

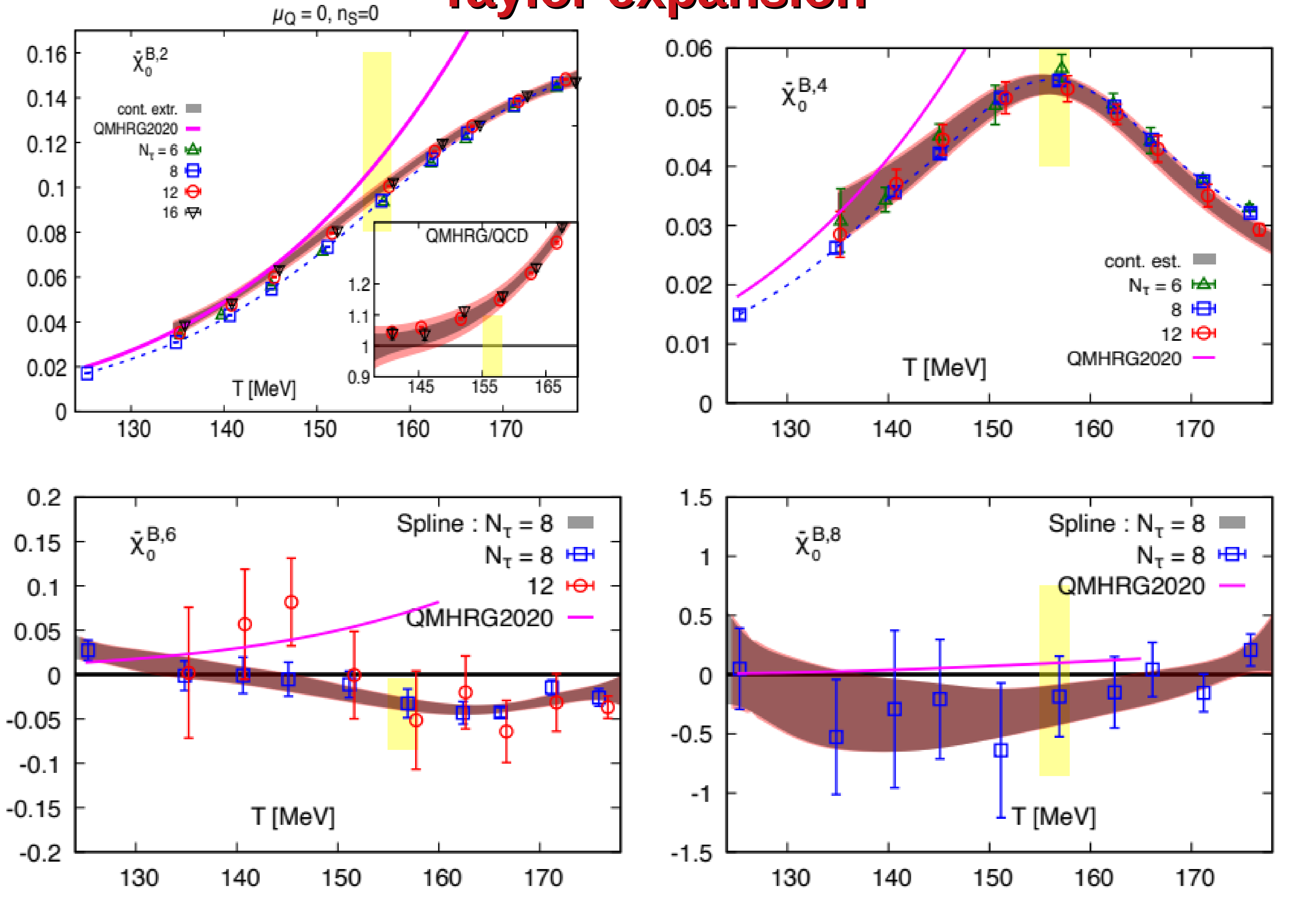

control basic features of skewness up to hyper-kurtosis ratios

A. Bazavov et al. (HotQCD), Phys. Rev. D 105 (2022) 074511 arXiv:2202.09184

2^{nd} order cumulants: fluctuations and correlations

two constraints: only 4 out of 6
2^{nd} order observables are independent

$T_c = (156.5 \pm 1.5)\mathrm{MeV}$

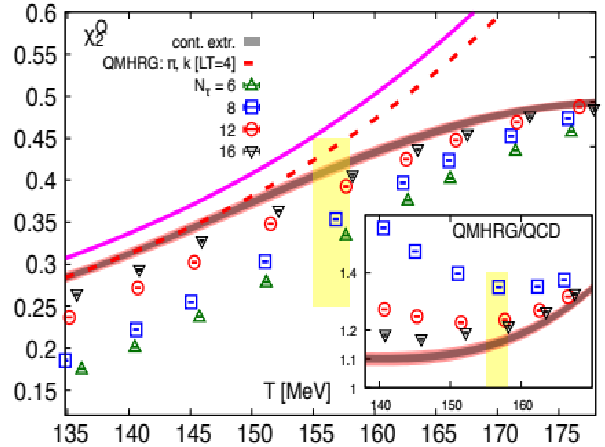

$$\chi_2^B = 2\chi_{11}^{BQ} - \chi_{11}^{BS} \qquad \chi_2^S = 2\chi_{11}^{QS} - \chi_{11}^{BS}$$

– **exact relations in QCD for**
– **satisfied in HRG models to better than 1%**

– **basic features:**

cumulants involving net electric charge differ earlier from HRG model calculations

cumulants involving strangeness agree with appropriately chosen HRG model up to T_{pc}

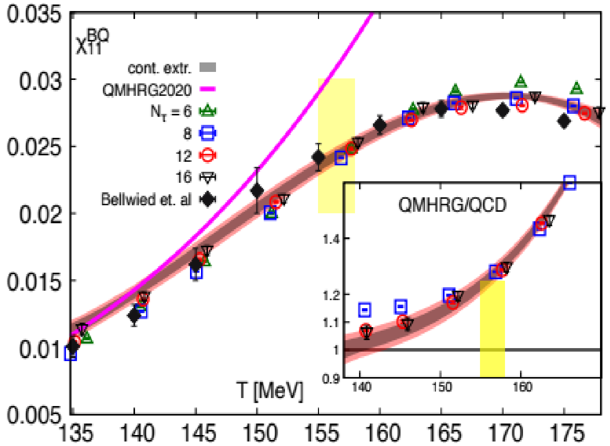

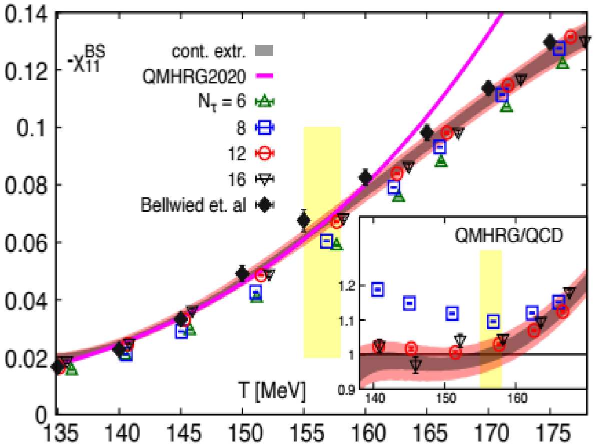

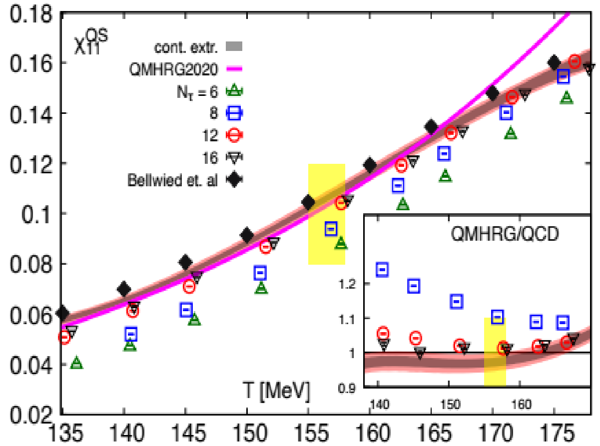

– continuum extrapolated results for all 2^{nd} order cumulants in (2+1)-flavor QCD

HotQCD (Jishnu Goswami), Phys.Rev.D 104 (2021) 074512 [arXiv:2107.10011}

Equation of state of (2+1)-flavor QCD: $\mu_B/T > 0$

$$\frac{\Delta p(T,\mu_B)}{T^4} = \frac{p(T,\mu_B) - p(T,0)}{T^4} = P_2(T)\left(\frac{\mu_B}{T}\right)^2 + P_4(T)\left(\frac{\mu_B}{T}\right)^4 + P_6(T)\left(\frac{\mu_B}{T}\right)^6 + \ldots$$

EoS 2017: $\mu_B = 0$

$\mu_B/T = 0$

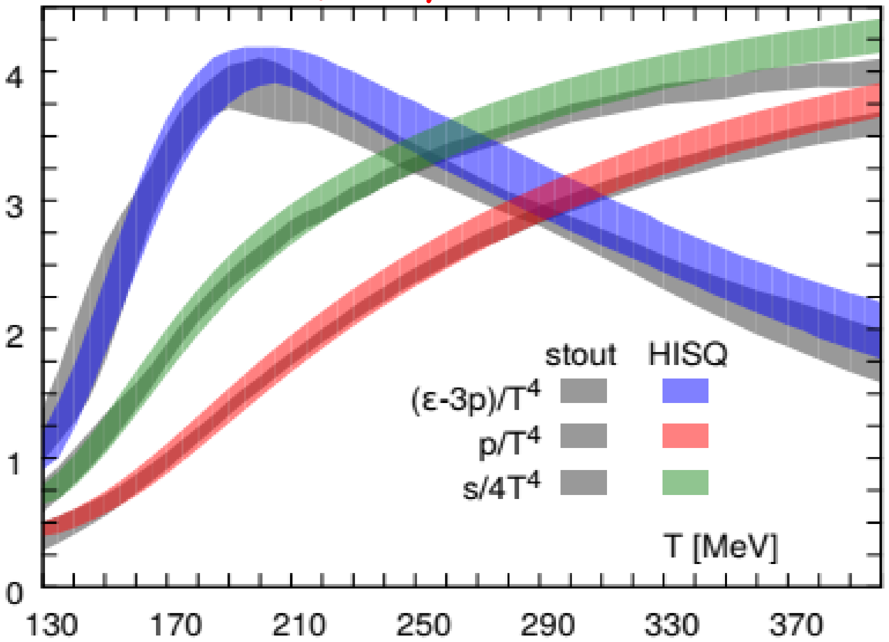

EoS 2022: non-zero μ_B **contribution**

$\mu_B/T = 2$ **:** (10-30)% contribution to total pressure at

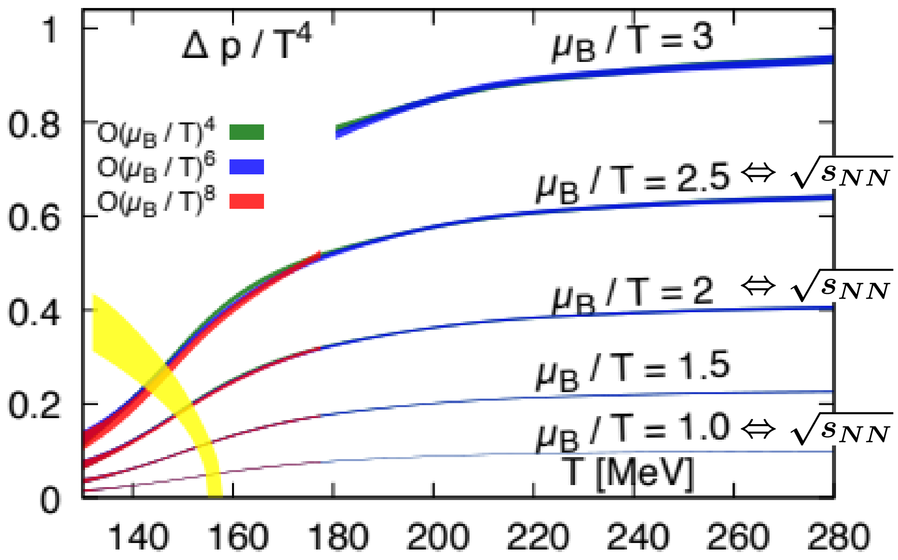

A. Bazavov et al (HotQCD), arXiv:1701.04325

D. Bollweg et al (HotQCD), arXiv:2212.09043

Higher order net baryon-number cumulant ratios on the pseudo-critical line

A. Bazavov et al. (HotQCD), PRD 101 (2020) 074502
PRD 96 (2017) 074510

constrained Taylor series, demanding strangeness neutrality:

$n_S = 0$ and $n_Q/n_B = 0.4$

$$\Rightarrow \quad R^B_{nm} = \frac{\chi^B_n(T,\mu_B)}{\chi^B_m(T,\mu_B)} = \frac{\sum_{k=1}^{k_{max}} \tilde{\chi}^{B,k}_n(T)\hat{\mu}^k_B}{\sum_{l=1}^{l_{max}} \tilde{\chi}^{B,l}_m(T)\hat{\mu}^l_B}$$

mean over variance

$$R^B_{12} = (M/\sigma^2)_B = \frac{\chi^B_1}{\chi^B_2}$$

– good QCD observable to relate "physical observable" to model dependent chemical potential

$\sqrt{s_{NN}} \sim 19.6$ GeV

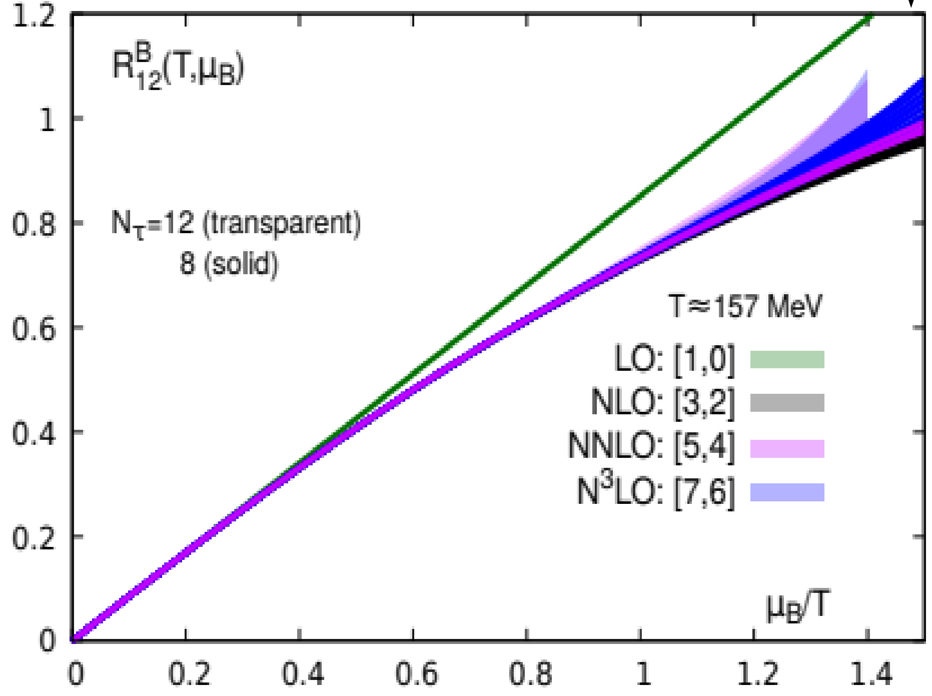

Higher order net baryon-number cumulant ratios on the pseudo-critical line

A. Bazavov et al. (HotQCD), PRD 101 (2020) 074502
PRD 96 (2017) 074510

constrained Taylor series, demanding strangeness neutrality:

$n_S = 0$ and $n_Q/n_B = 0.4$

$$R^B_{nm} = \frac{\chi^B_n(T,\mu_B)}{\chi^B_m(T,\mu_B)} = \frac{\sum_{k=1}^{k_{max}} \tilde{\chi}^{B,k}_n(T)\hat{\mu}^k_B}{\sum_{l=1}^{l_{max}} \tilde{\chi}^{B,l}_m(T)\hat{\mu}^l_B}$$

$\sqrt{s_{NN}} \sim 19.6$ GeV

mean over variance

$$R^B_{12} = (M/\sigma^2)_B = \frac{\chi^B_1}{\chi^B_2}$$

– good QCD observable to relate "physical observable" to model dependent chemical potential

– weak temperature dependence

comtinuum limit estimate

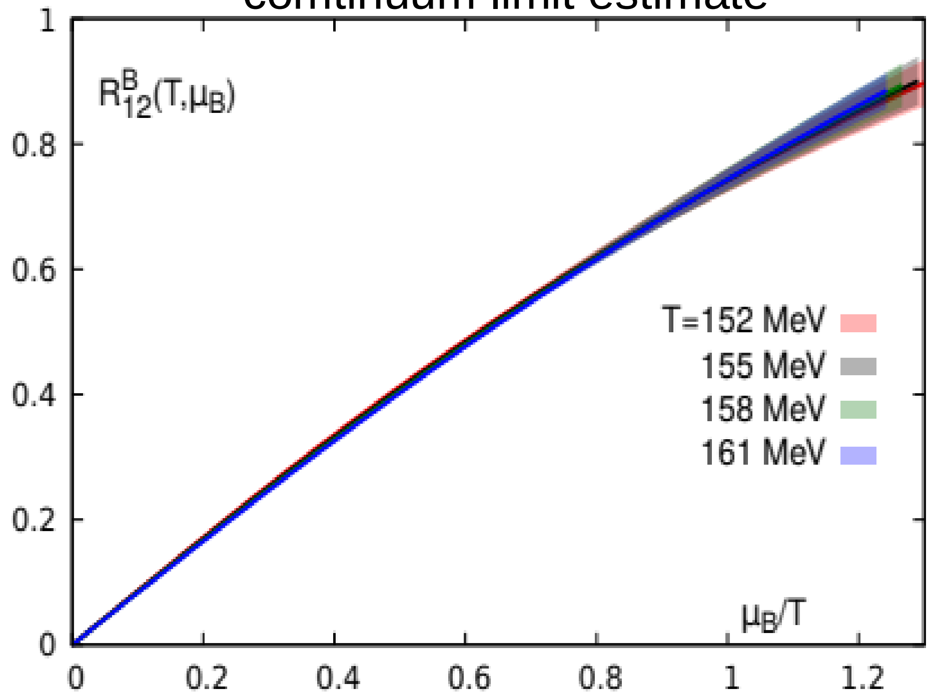

Higher order net baryon-number cumulant ratios on the pseudo-critical line

A. Bazavov et al. (HotQCD), PRD 101 (2020) 074502
PRD 96 (2017) 074510

constrained Taylor series, demanding strangeness neutrality:

$n_S = 0$ and $n_Q/n_B = 0.4$

$$R^B_{nm} = \frac{\chi^B_n(T,\mu_B)}{\chi^B_m(T,\mu_B)} = \frac{\sum_{k=1}^{k_{max}} \tilde{\chi}^{B,k}_n(T)\hat{\mu}^k_B}{\sum_{l=1}^{l_{max}} \tilde{\chi}^{B,l}_m(T)\hat{\mu}^l_B}$$

new STAR data on proton-number ratio $R^p_{12}(\sqrt{s_{NN}})$ presented at CPOD 2024 by A. Pandav

mean over variance

$$R^X_{12} = (M/\sigma^2)_X = \frac{\chi^X_1}{\chi^X_2}$$

X=B (QCD)
P (STAR)

– used STAR results on hadron yields to convert $\sqrt{s\_NN} \Leftrightarrow \mu_B$

L. Adamczyk (STAR), PRC 96 (2017) 044904

– **thermal conditions determined from STAR proton cumulants at freeze-out are consistent with those determined in QCD from baryon cumulants on the pseudo-critical line**

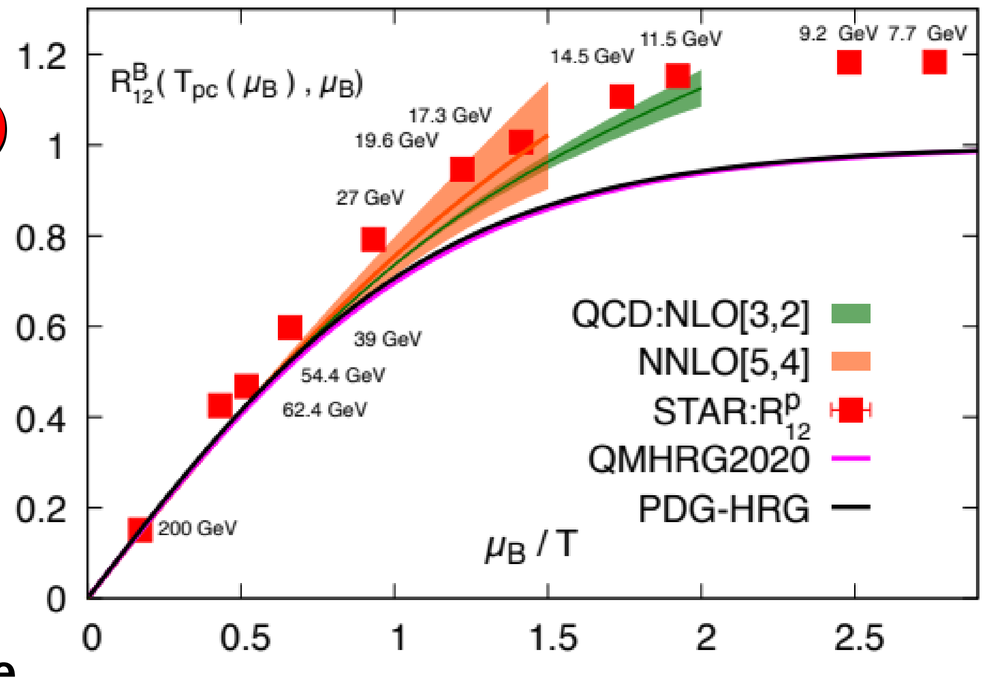

D. Bollweg et al., arXiv:2407.09335

Higher order cumulant ratios on the pseudo-critical line

A. Bazavov et al. (HotQCD), PRD 101 (2020) 074502
PRD 96 (2017) 074510

skewness

$$R_{31}^B = \left(\frac{S\sigma^3}{M}\right)_B = \frac{\chi_3^B}{\chi_1^B}$$

kurtosis

$$R_{42}^B = (\kappa\sigma^2)_B = \frac{\chi_4^B}{\chi_2^B}$$

$\mathcal{O}(\mu_B^4)$ Taylor series ⟺ $\mathcal{O}(\mu_B^8)$ Taylor series for pressure

$$R_{nm}^B = \frac{\chi_n^B(T,\mu_B)}{\chi_m^B(T,\mu_B)} = \frac{\sum_{k=1}^{k_{max}} \tilde{\chi}_n^{B,k}(T)\hat{\mu}_B^k}{\sum_{l=1}^{l_{max}} \tilde{\chi}_m^{B,l}(T)\hat{\mu}_B^l}$$

$$n_S = 0,\ n_Q/n_B = 0.4$$

$$R_{31}^B(T,\mu_B) = r_{31}^{B,0}(T) + r_{31}^{B,2}(T)\left(\frac{\mu_B}{T}\right)^2 + \mathcal{O}(\mu_B^4)$$

$$R_{42}^B(T,\mu_B) = r_{42}^{B,0}(T) + r_{42}^{B,2}(T)\left(\frac{\mu_B}{T}\right)^2 + \mathcal{O}(\mu_B^4)$$

$\mu_S = \mu_Q = 0$

$$r_{42}^{B,0} = r_{31}^{B,0}$$

$$r_{42}^{B,2} = 3 r_{31}^{B,2}$$

$n_S = 0,\ n_Q/n_B = 0.4$

$$\frac{r_{42}^{B,0}}{r_{31}^{B,0}} = \frac{1 + s_1 \frac{\chi_{11}^{BS}}{\chi_2^B} + q_1 \frac{\chi_{11}^{BQ}}{\chi_2^B}}{1 + s_1 \frac{\chi_{31}^{BS}}{\chi_4^B} + q_1 \frac{\chi_{31}^{BQ}}{\chi_4^B}}$$

$T_{pc}(\mu_B) = T_0(1 - \kappa_2^f(\mu_B/T)^2)$

$$r_{nm}^{B,k} \rightarrow r_{nm,f}^{B,k} \equiv r_{nm}^{B,k}(T_0) - \kappa_2^f T_0 \left.\frac{\mathrm{d}r_{nm}^{B,k-2}}{\mathrm{d}T}\right|_{T=T_0}$$

HotQCD, Phys.Rev.D 96 (2017) 074510, arXiv:1708.04897

Higher order cumulant ratios on the pseudo-critical line

A. Bazavov et al. (HotQCD), PRD 101 (2020) 074502
PRD 96 (2017) 074510

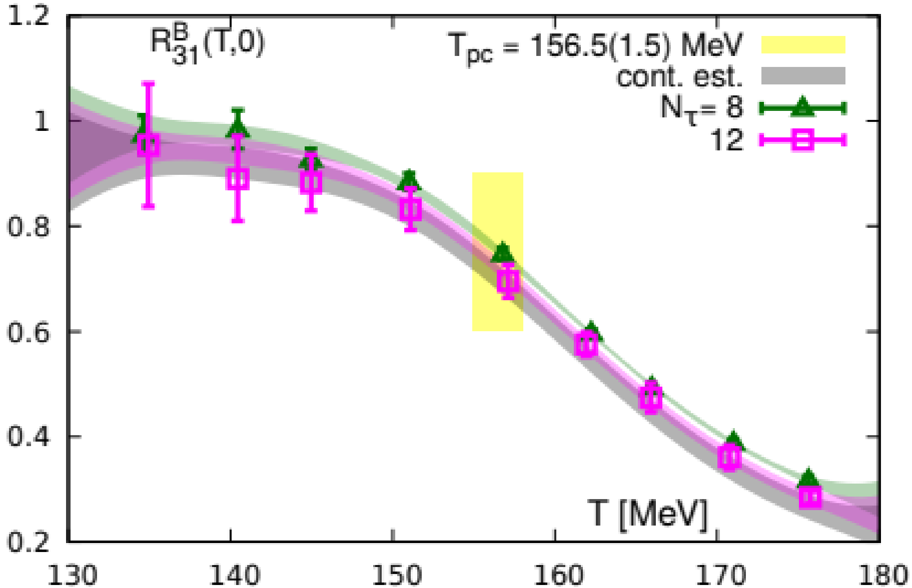

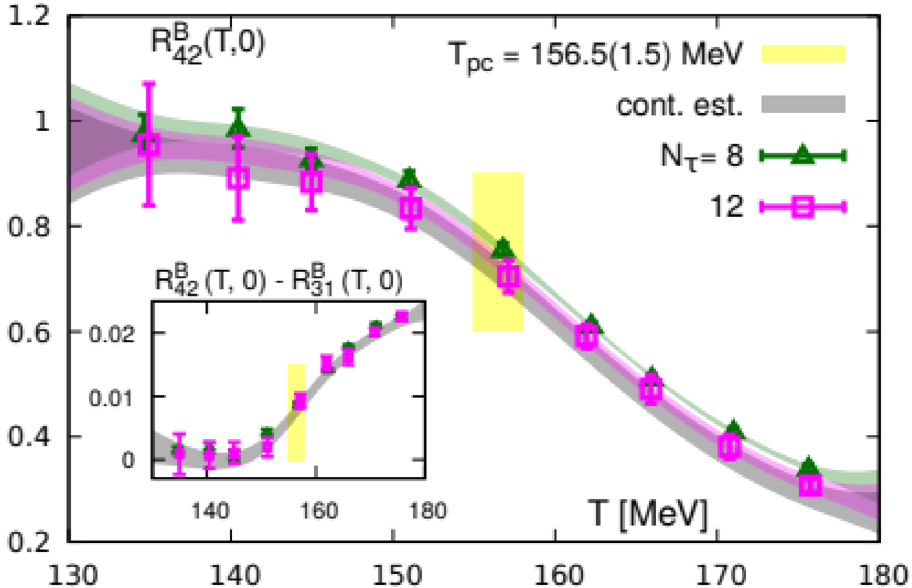

$$n_S = 0,\ n_Q/n_B = 0.4$$

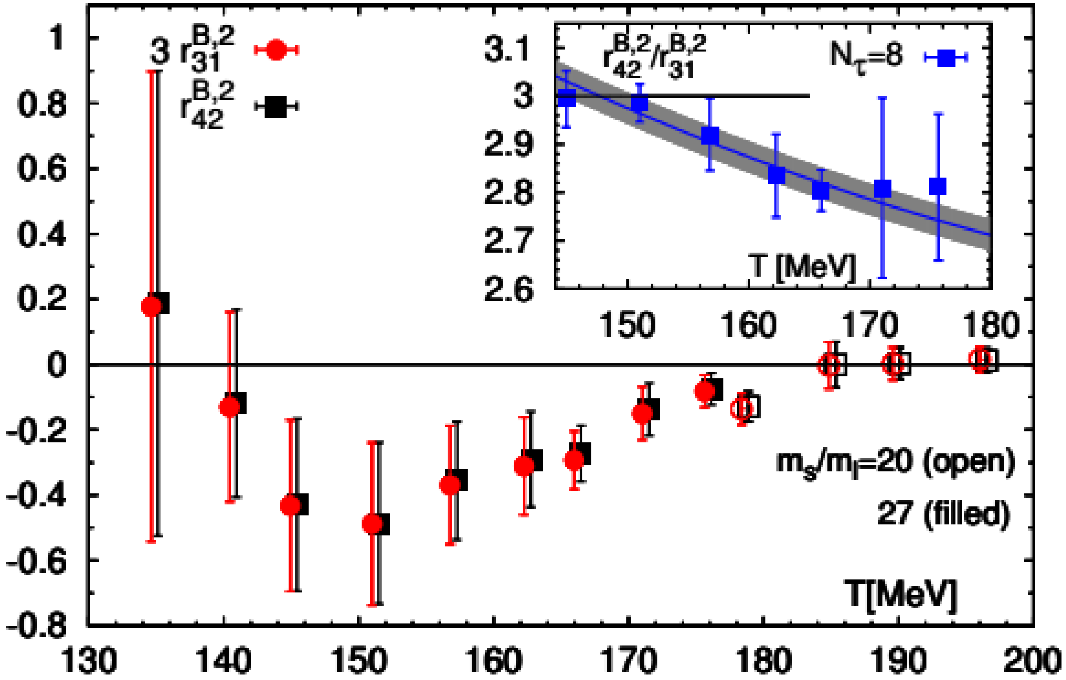

$$\mu_S = \mu_Q = 0$$

$$r^{B,0}_{42} = r^{B,0}_{31}$$

$$r^{B,2}_{42} = 3 r^{B,2}_{31}$$

still well fulfilled also for

$$n_S = 0$$

$$n_Q/n_B = 0.4$$

Higher order cumulant ratios on the pseudo-critical line

A. Bazavov et al. (HotQCD), PRD 101 (2020) 074502
PRD 96 (2017) 074510

skewness

$$R_{31}^B = \left(\frac{S\sigma^3}{M}\right)_B = \frac{\chi_3^B}{\chi_1^B}$$

kurtosis

$$R_{42}^B = (\kappa\sigma^2)_B = \frac{\chi_4^B}{\chi_2^B}$$

$$n_S = 0,\ n_Q/n_B = 0.4$$

$\mathcal{O}(\mu_B^4)$ Taylor series ⟺ $\mathcal{O}(\mu_B^8)$ Taylor series for pressure

$$R_{nm}^B = \frac{\chi_n^B(T,\mu_B)}{\chi_m^B(T,\mu_B)} = \frac{\sum_{k=1}^{k_{max}} \tilde{\chi}_n^{B,k}(T)\hat{\mu}_B^k}{\sum_{l=1}^{l_{max}} \tilde{\chi}_m^{B,l}(T)\hat{\mu}_B^l}$$

also at NNLO curvature of R_{42}^B is about a factor 3 larger than that of R_{31}^B

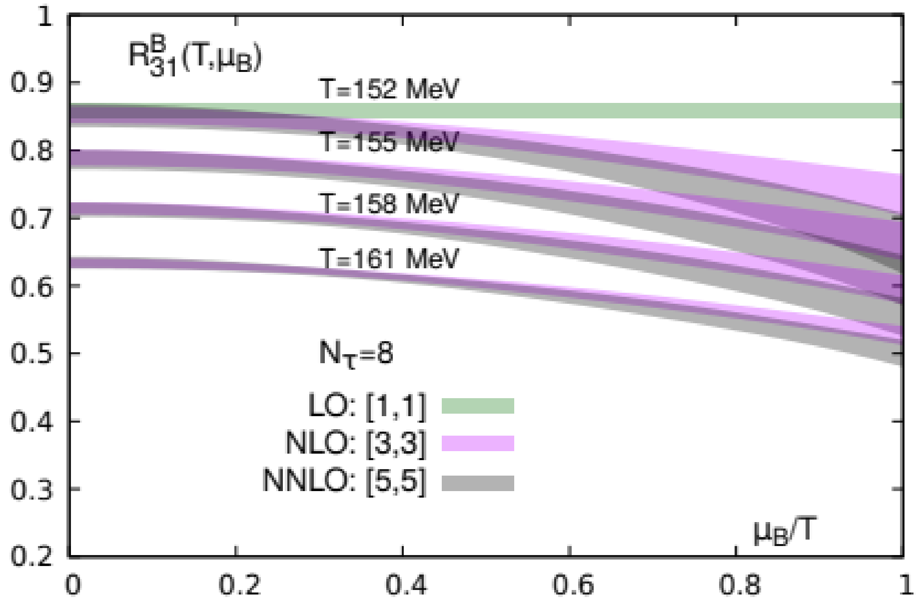

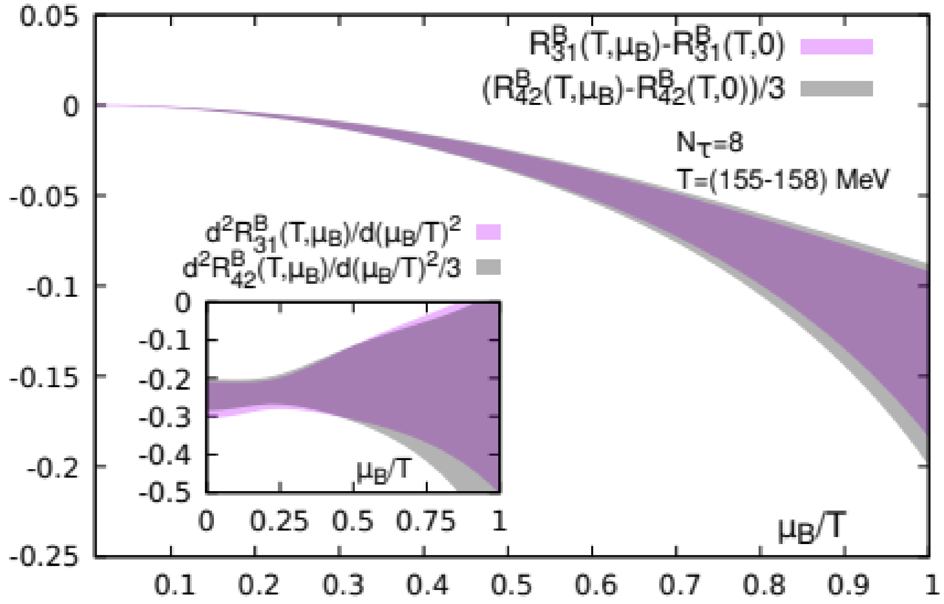

Skewness and kurtosis ratios

QCD on the pseudo-critical line vs. STAR data at freeze-out

$\mathcal{O}(\mu_B^4)$ QCD for $n_S = 0,\ n_Q/n_B = 0.4$
on the pseudo-critical line

new STAR data:
presented at CPOD 2024
by A. Pandav

$\underline{\mu_B = 0}$

$$\left.\frac{\chi_4^B}{\chi_2^B}\right|_{T_{pc}(0)} = 0.69(3)$$

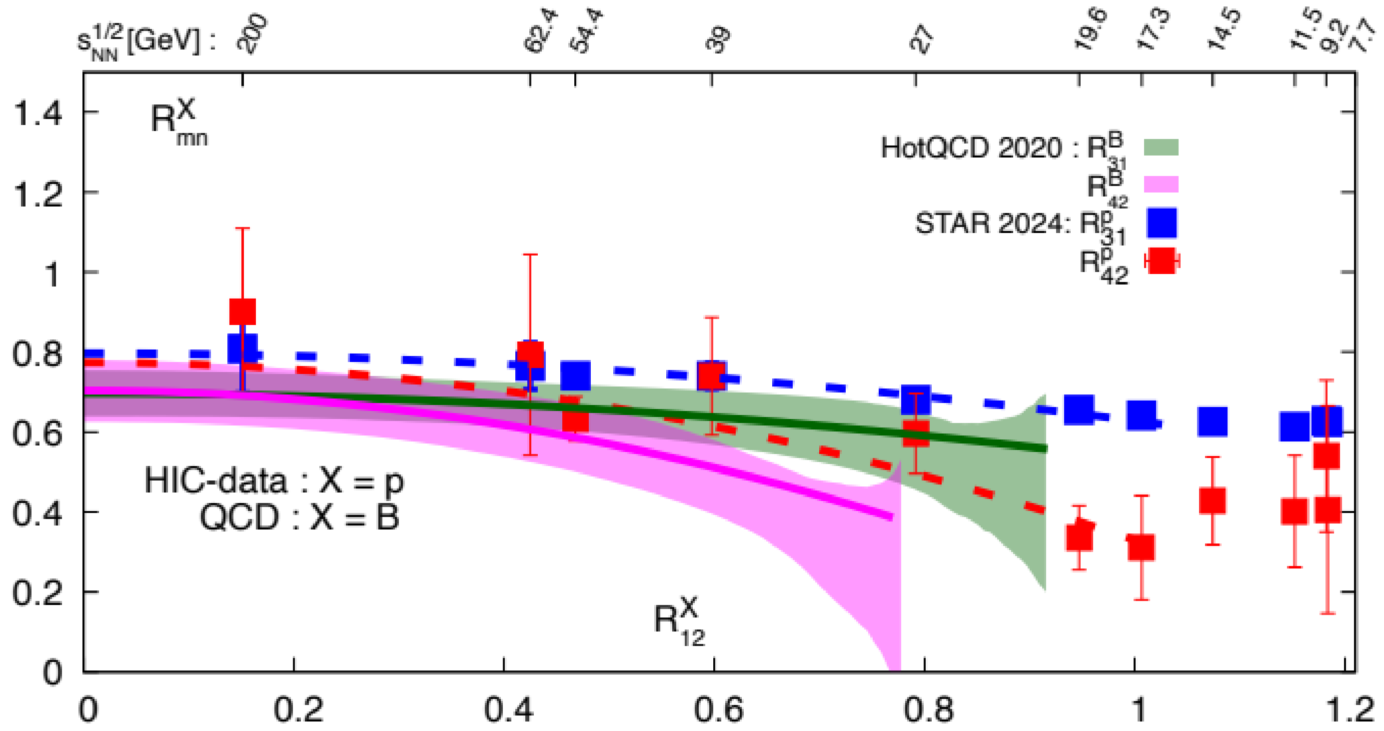

STAR, CPOD 2024

$$R_{31}^p = 0.80(1) - 0.17(2)\,(R_{12}^p)^2$$

$$R_{42}^p = 0.77(6) - 0.44(12)\,(R_{12}^p)^2$$

fit for $0 \le R_{12}^p \le 1$

HotQCD 2017, 2020:

$$R_{31}^B = 0.70(1) - 0.169(2)\left(R_{12}^B\right)^2$$

$$R_{42}^B = 0.705(1) - 0.556(2)\left(R_{12}^B\right)^2$$

fit for $0 \le R_{12}^B \le 0.5$

Conclusions

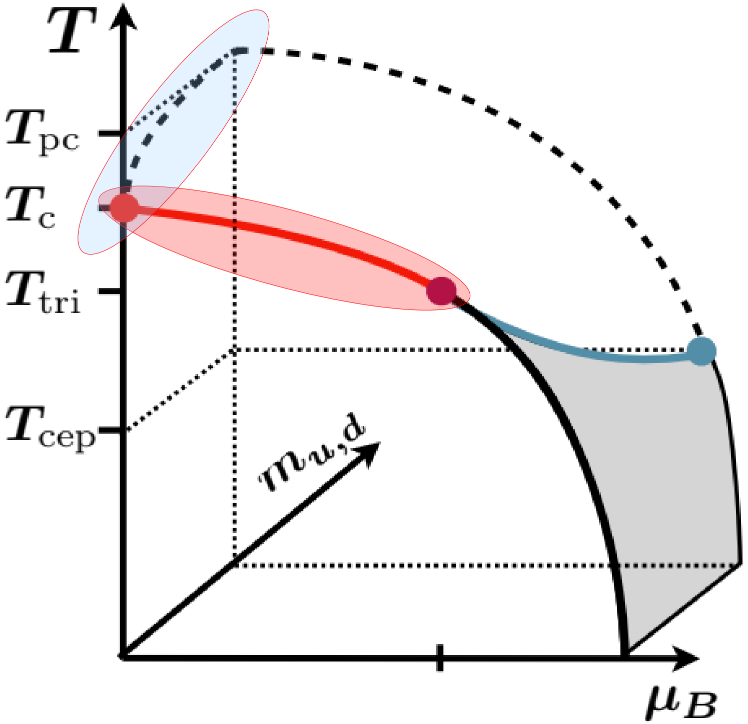

What we learned so far about the CEP in QCD from lattice QCD calculations:

I) the critical temperature is below $T_c = 132^{+3}_{-6}$ MeV

II) the corresponding critical chemical potential is likely to be above 500 MeV

⟶ Taylor expansions need to be resummed in order to reach higher μ_B/T

– no CEP for $\mu_B/T \le 2.5$

– CEP not in the BES-II range (in collider mode)

– EoS (pressure & number density) well controlled for

$\mu_B/T \le 2.0 \ \forall T > 135$ MeV

(larger range for higher T)

– reliable μ_B - range is smaller for higher order cumulants, given only an 8th order Taylor series for the pressure

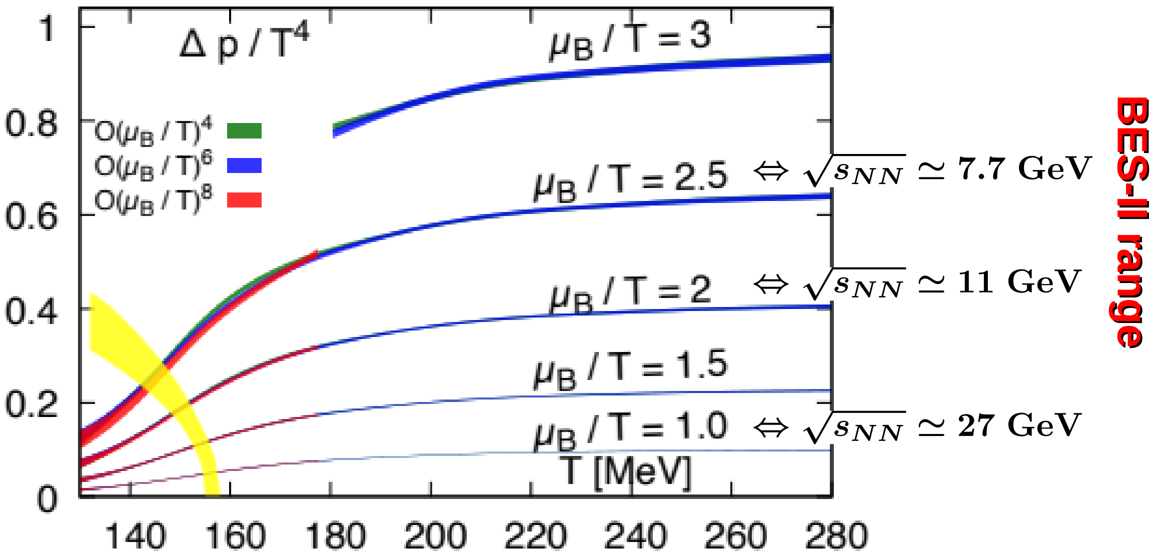

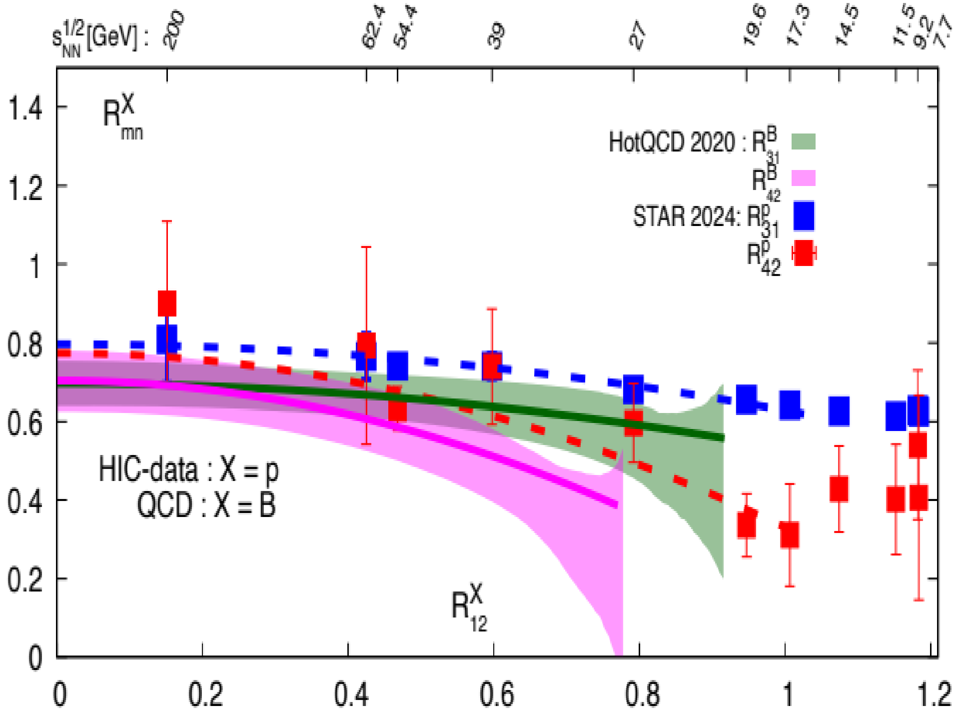

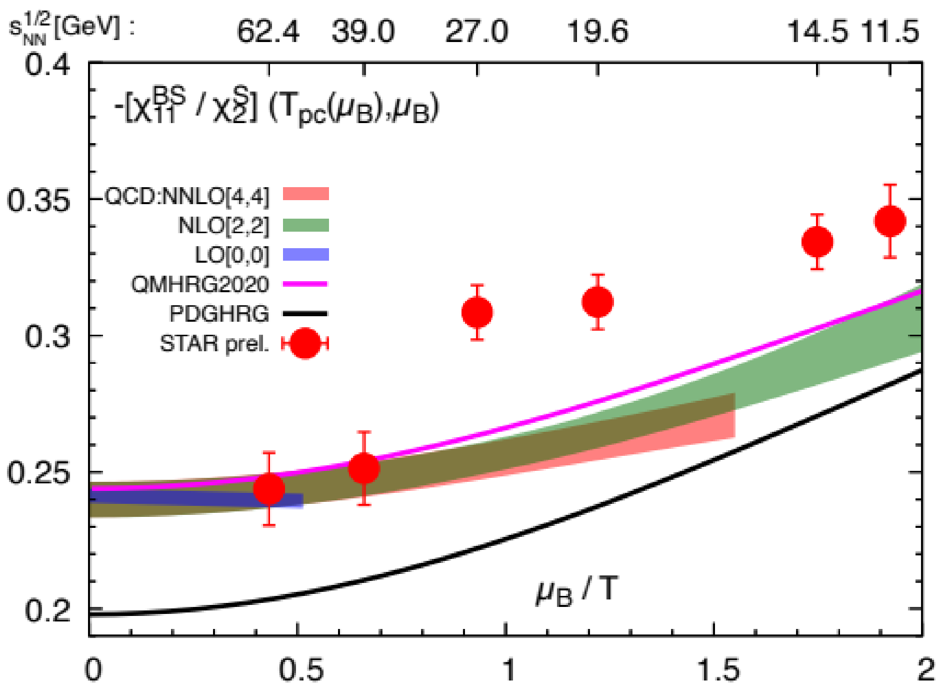

Skewness and kurtosis ratios

- QCD and STAR results are in good agreement for $\sqrt{s_{NN}} \geq \mathbf{19.6}$ GeV
- $\mathcal{O}((R_{12}^B)^2)$ QCD results and quadratic fit to STAR results for R_{31}^p and R_{42}^p agree well on curvature coefficient.
- difference in LO coefficients may suggest that freeze-out temperature is slightly below T_{pc}.

Baryon number – Strangeness correlations

- QCD and STAR results are in good agreement for $\sqrt{s_{NN}} \geq \mathbf{39}$ GeV
- Significant differences between QCD and STAR results for $\sqrt{s_{NN}} \leq \mathbf{27}$ GeV
- Good agreement between QCD, QMHRG2020 and STAR data for large $\sqrt{s_{NN}}$ suggest sensitivity of data to missing baryon resonances, which requires careful handling of feed-down corrections

Baryon number – strangeness correlations
HIC at freeze-out vs. QCD on the pseudo-critical line

QCD Taylor series up to $\mathcal{O}((\mu_B/T)^4)$
compared with preliminary STAR data

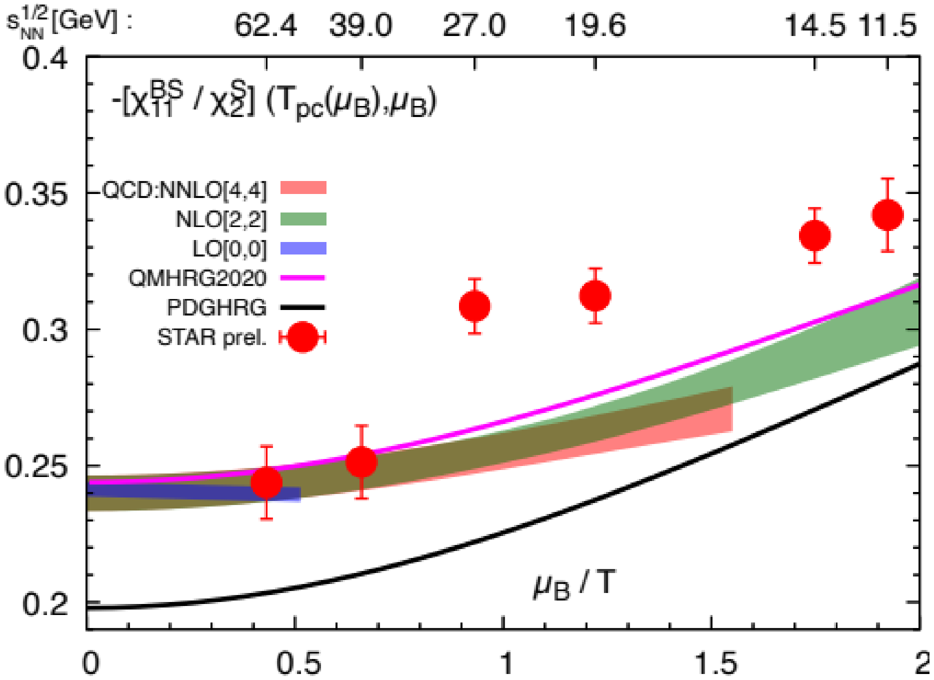

H.W. Feng (STAR), CPOD 2024

D. Bollweg, H.-T. Ding, J.Goswami, FK,
Swagato Mugherjee, P. Petreczky, C. Schmidt,
arXiv:2407.09335

strangeness-electric charge
correlations

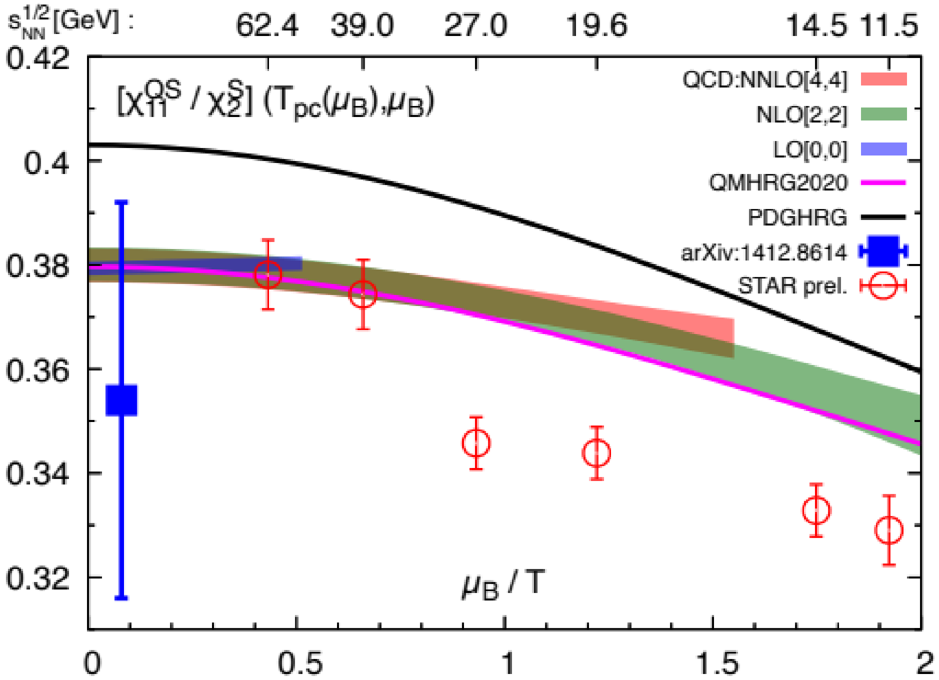

using that isospin violations
are small in QCD:

$$2\frac{\chi_{11}^{QS}}{\chi_2^S} + \frac{\chi_{11}^{BS}}{\chi_2^S} \simeq 1$$

holds to better than 1%

Ratio of baryon number – strangeness correlation and net strangeness fluctuations

$$\frac{\mu_S}{\mu_B} \equiv -\frac{\chi_{11}^{BS}}{\chi_2^S} - q_1 \frac{\chi_{11}^{QS}}{\chi_2^S} + \mathcal{O}(\mu_B^2)$$

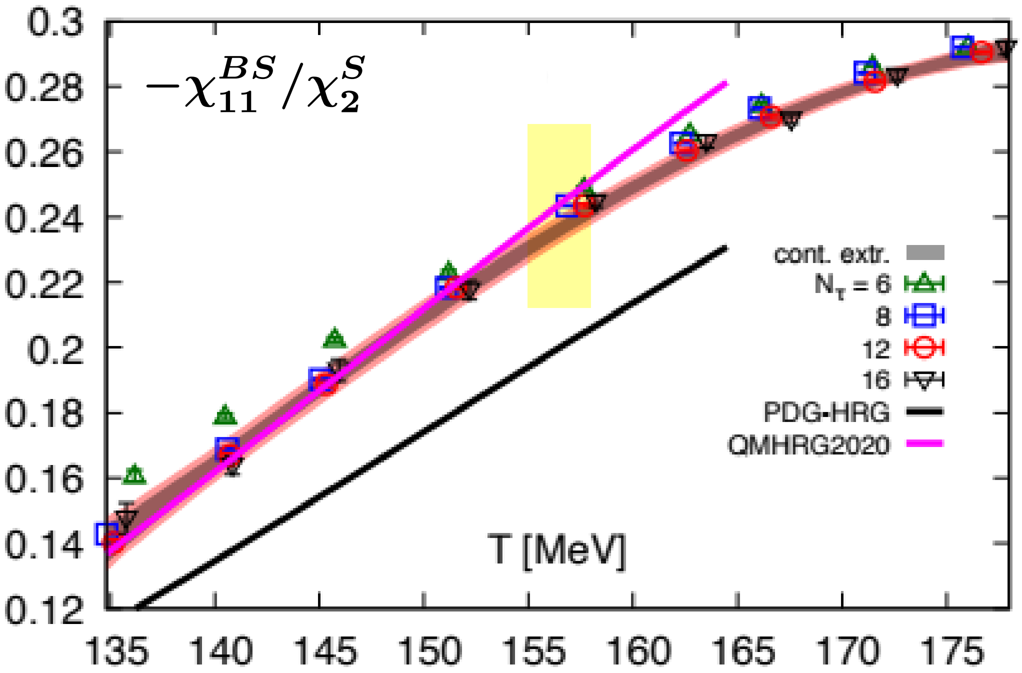

- evidence for experimentally not yet observed strange baryons?
- evidence for strong flavor correlations

$$-\frac{\chi_{11}^{BS}}{\chi_2^S} = \frac{1}{3} + \frac{2}{3}\frac{\chi_{11}^{us}}{\chi_2^s}$$

D. Bollweg et al. (HotQCD), arXiv:2107.10011

PDG-HRG: uses experimentally known hadron spectrum listed by the Particle Data Group
QM-HRG: uses additional hadrons predicted to exist in Quark Model calculations

Ratio of baryon number – strangeness correlation and net strangeness fluctuations

$$\frac{\mu_S}{\mu_B} \equiv -\frac{\chi_{11}^{BS}}{\chi_2^S} - q_1 \frac{\chi_{11}^{QS}}{\chi_2^S} + \mathcal{O}(\mu_B^2)$$

$$\left.\frac{\mu_S}{\mu_B}\right|_{T_{pc}(\mu_B)}$$ on the pseudo-critical line

$\mu_B = 0$

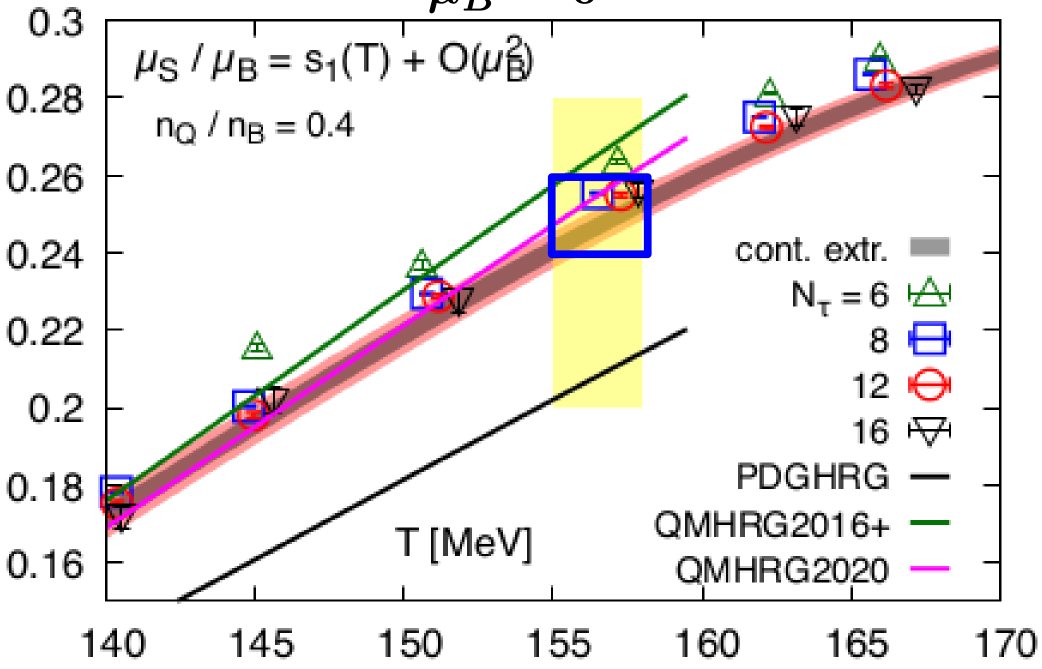

$\mu_B > 0$

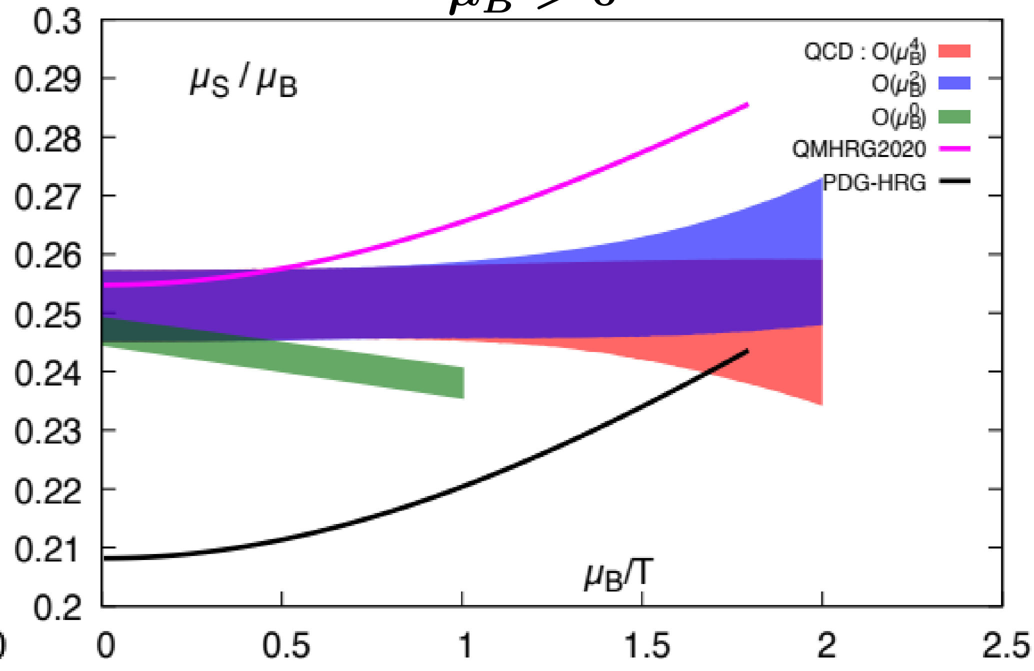

HotQCD, arXiv:2107.10011

at T_{pc} QCD: $-\chi_{11}^{BS}/\chi_2^S = 0.236(11)$

$$-q_1\chi_{11}^{QS}/\chi_2^S = 0.009(1)$$

for $n_Q/n_B = 0.4 \Rightarrow \frac{\mu_S}{\mu_B} = 0.245(11)$

on $T_{pc}(\mu_B)$: Taylor series converges well up to $\mu_B/T \simeq 2$

deviations from QMHRG increase with increasing μ_B/T: O(10%) at $\mu_B/T \simeq 2$

Freeze-out parameter from strange baryon yields

STAR2020: Phys. Rev. C 102 (2020) 034909

data are consistent with HRG-model ansatz: $Y_H \sim \mathrm{e}^{(B\mu_B + Q\mu_Q + S\mu_S)/T}$

Determination of freeze-out parameters by comparing ratios of multi-strange baryon yields with HRG-motivated Boltzmann ansatz $\ln(\overline{\mathrm{B}}/\mathrm{B}) = -2\mu_B/T_{\mathrm{ch}} + \mu_S/T_{\mathrm{ch}} \cdot \Delta S$

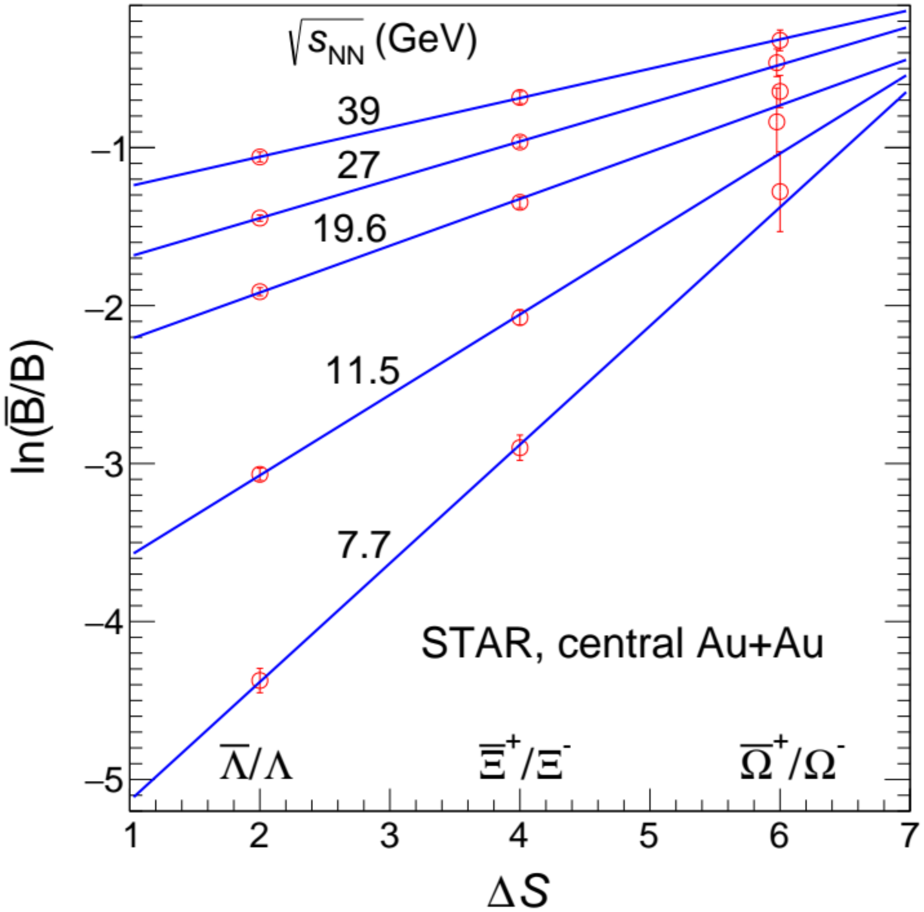

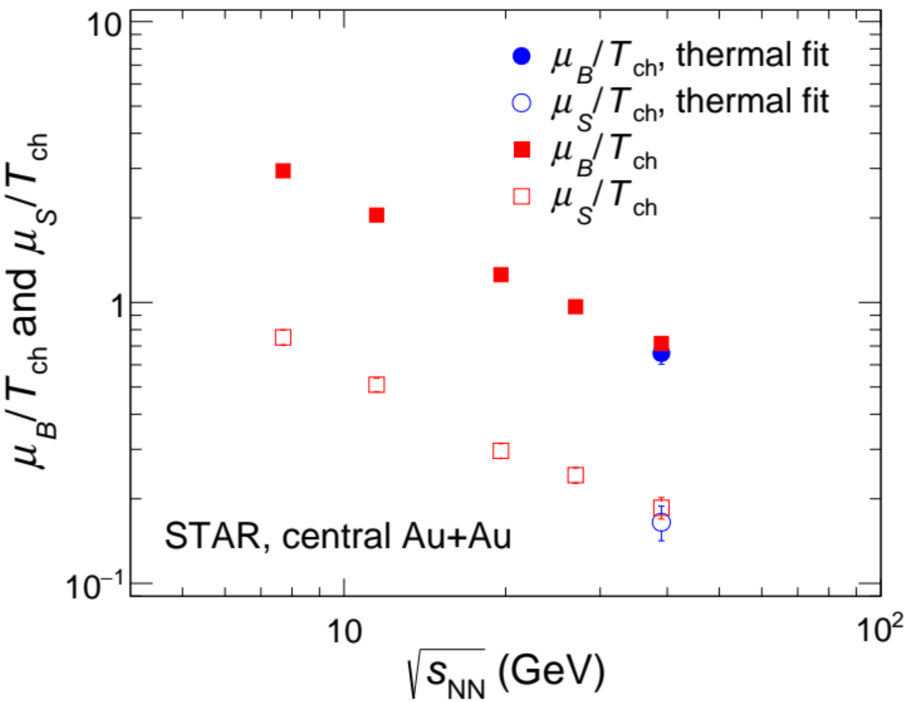

Baryon number – strangeness chemical potentials at freeze-out from strange baryon yields vs. QCD

QCD:

$$\frac{\mu_S}{\mu_B} \equiv -\frac{\chi_{11}^{BS}}{\chi_2^S} - q_1 \frac{\chi_{11}^{QS}}{\chi_2^S} + \mathcal{O}(\mu_B^2)$$

STAR:

$$\ln(\overline{\mathrm{B}}/\mathrm{B}) = -2\mu_B/T_{\mathrm{ch}} + \mu_S/T_{\mathrm{ch}} \cdot \Delta S$$

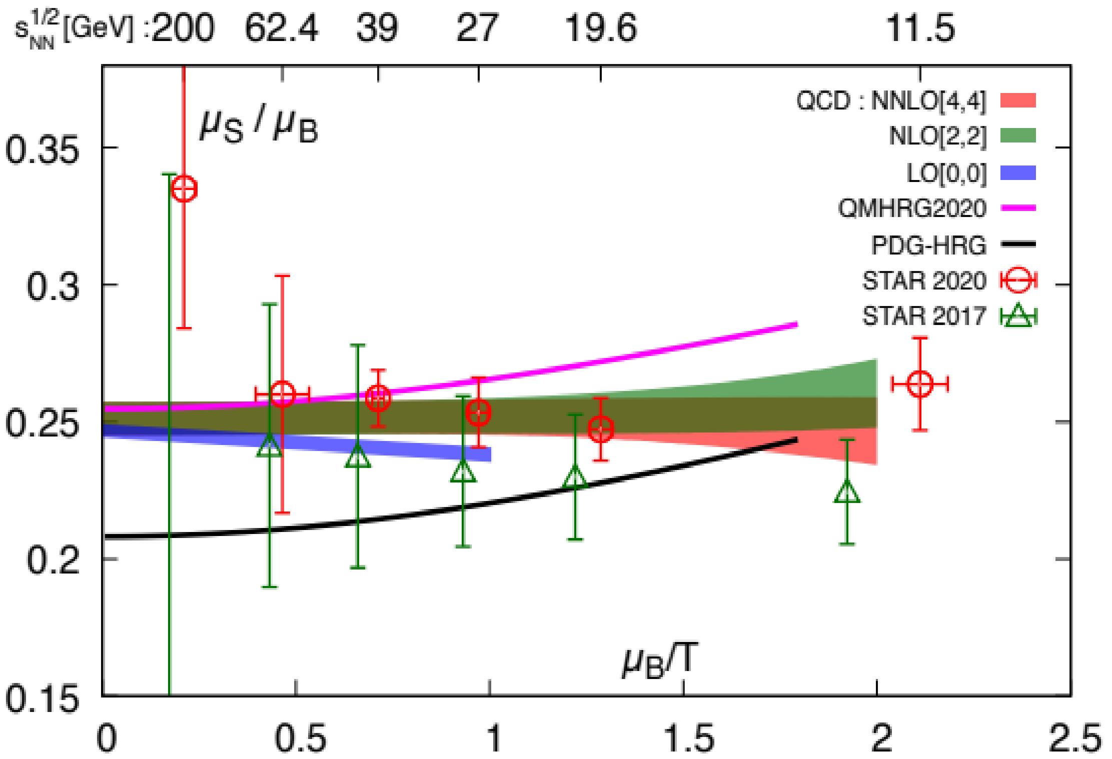

HotQCD, Phys. Rev. D 104 (2021) 074512
arXiv:2107.10011

STAR2017: Phys. Rev. C 96 (2017) 044904
STAR2020: Phys. Rev. C 102 (2020) 034909

STAR multi-strange baryon yields are consistent with freeze-out at T_{pc} and a μ_S/μ_B that reflects contributions from additional strange baryons

The Chiral PHASE TRANSITION in (2+1)-flavor QCD

$$M \sim m_s \partial \ln Z / \partial m_l$$

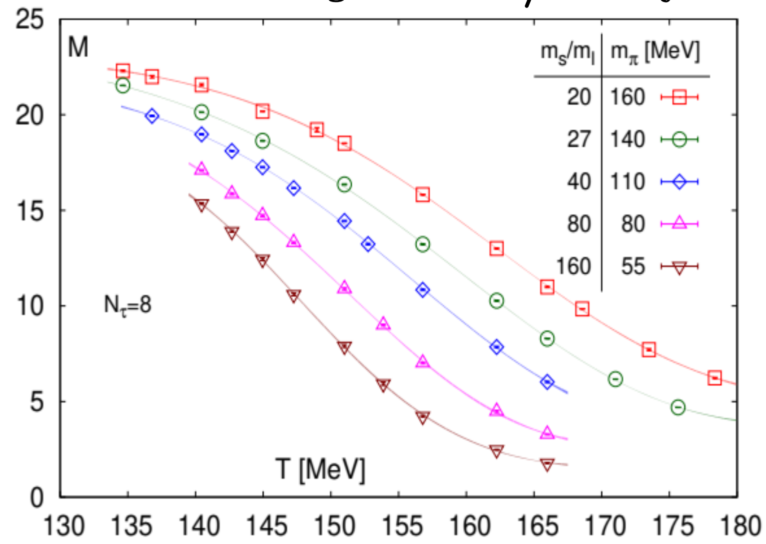

m_s fixed, physical

$m_l \Rightarrow 0$

"magnetic" susceptibility

$$\chi_M \sim \frac{\partial^2 \ln Z}{\partial m_l^2}$$

$$\sim (m_s/m_l)^{0.79}$$

$$(160/27)^{0.79} \sim 4$$

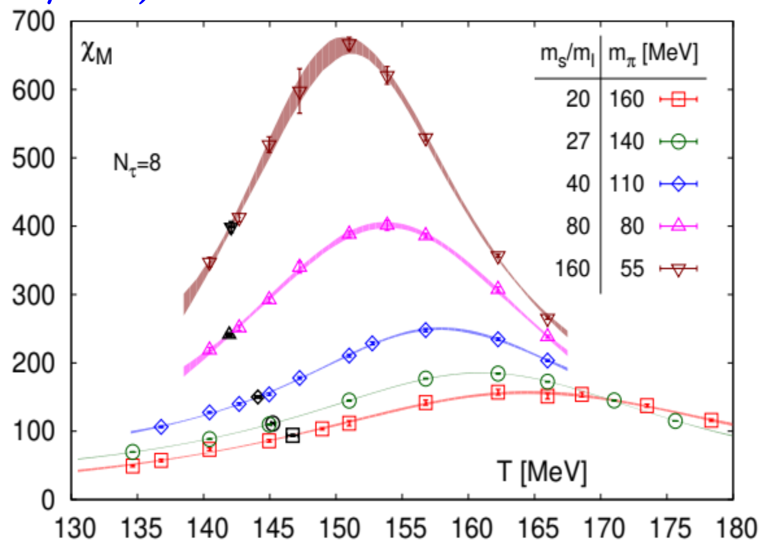

"mixed" susceptibility

$$\chi_t \sim \frac{\partial^2 \ln Z}{\partial T \partial m_l}$$

$$\sim (m_s/m_l)^{0.34}$$

$$(160/27)^{0.34} \sim 1.8$$

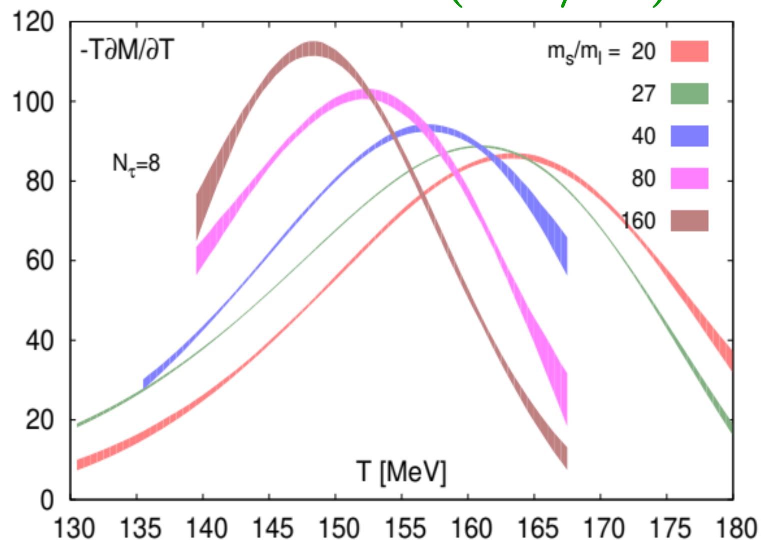

H.T. Ding et al. (HotQCD), PRL 123 (2019) 15, arXiv:1903.04801

The Chiral PHASE TRANSITION in (2+1)-flavor QCD

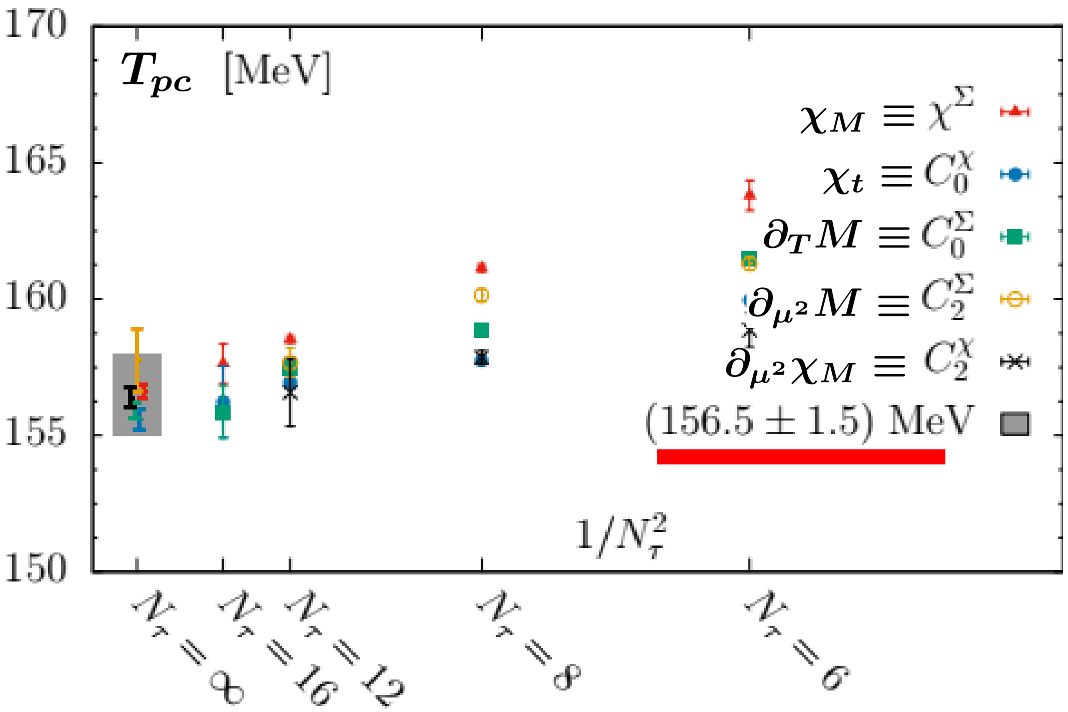

A. Bazavov et al (HotQCD), arXiv:1812.08235

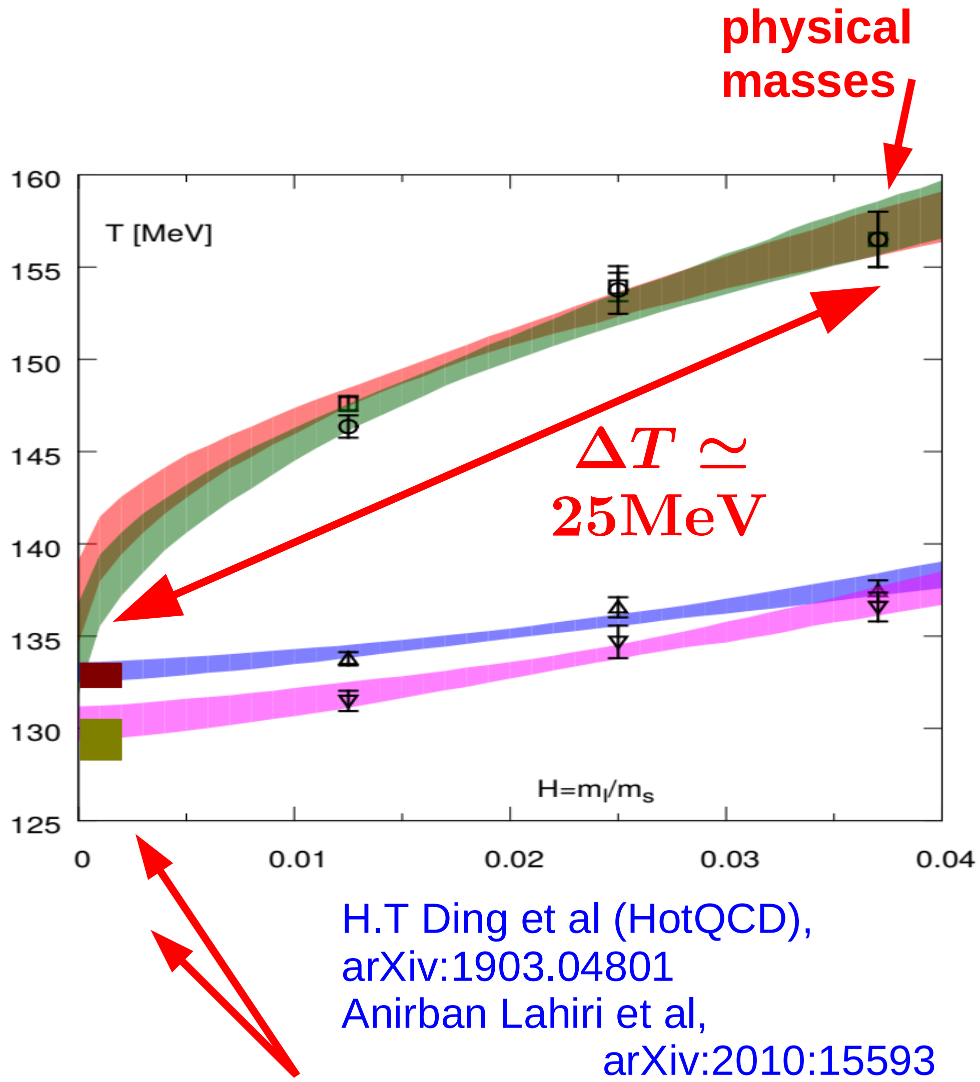

H.T Ding et al (HotQCD), arXiv:1903.04801
Anirban Lahiri et al, arXiv:2010:15593

physical masses

$$T_{pc}^{phys} = (156.5 \pm 1.5)\ \text{MeV}$$

chiral limit extrapolations

$$T_c^0 = 132^{+3}_{-6}\ \text{MeV}$$